



A natural symbiotic bacterium drives mosquito refractoriness to *Plasmodium* infection via secretion of an antimalarial lipase

Han Gao^{1,2,8}, Liang Bai^{1,2,8}, Yongmao Jiang^{1,2}, Wei Huang³, Lili Wang^{1,2}, Shengguo Li⁴, Guoding Zhu⁵, Duoquan Wang⁶, Zhenghui Huang⁷, Xishang Li⁴, Jun Cao¹, Lubing Jiang⁷, Marcelo Jacobs-Lorena³, Shuai Zhan¹ and Sibao Wang^{1,2} ⊠

The stalling global progress in the fight against malaria prompts the urgent need to develop new intervention strategies. Whilst engineered symbiotic bacteria have been shown to confer mosquito resistance to parasite infection, a major challenge for field implementation is to address regulatory concerns. Here, we report the identification of a *Plasmodium*-blocking symbiotic bacterium, *Serratia ureilytica* Su_YN1, isolated from the midgut of wild *Anopheles sinensis* in China that inhibits malaria parasites via secretion of an antimalarial lipase. Analysis of *Plasmodium vivax* epidemic data indicates that local malaria cases in Tengchong (Yunnan province, China) are significantly lower than imported cases and importantly, that the local vector *A. sinensis* is more resistant to infection by *P. vivax* than *A. sinensis* from other regions. Analysis of the gut symbiotic bacteria of mosquitoes from Yunnan province led to the identification of *S. ureilytica* Su_YN1. This bacterium renders mosquitoes resistant to infection by the human parasite *Plasmodium falciparum* or the rodent parasite *Plasmodium berghei* via secretion of a lipase that selectively kills parasites at various stages. Importantly, Su_YN1 rapidly disseminates through mosquito populations by vertical and horizontal transmission, providing a potential tool for blocking malaria transmission in the field.

alaria remains one of the world's deadliest infectious diseases¹. As a malaria vaccine is not yet available, the use of insecticides against vector mosquitoes and antimalarial drugs to treat infection remain the mainstay of current malaria control programmes². However, the increasing incidence of mosquito insecticide resistance^{3,4} as well as parasite resistance to artemisinin and piperaquine⁵⁻⁸ have stalled the progress against malaria over the past few years. The number of malaria cases increased from 217 million in 2016 to 219 million in 2017 and 228 million in 2018 (ref. ¹). New intervention strategies to control this deadly infectious disease are urgently needed^{9,10}.

Malaria parasites are transmitted to humans through the bite of infected female *Anopheles* mosquitoes¹¹. For successful transmission, *Plasmodium* parasites must complete a complex developmental programme in the mosquito midgut¹², where the majority of ingested parasites are killed¹³⁻¹⁵, making the midgut compartment a prime target for intervention. *Anopheles* vector competence varies at both the species and individual level¹⁶, suggesting that both genetic and environmental factors affect the resistance of *Anopheles* mosquitoes to *Plasmodium* infection¹⁷. The mosquito gut is colonialized with various microorganisms, mostly Gram-negative bacteria^{12,18,19}. The midgut microbiota plays a critical role in modulating the outcome of *Plasmodium* infection in mosquitoes¹⁹⁻²² but the molecular mechanisms by which the gut symbiotic bacteria affect *Plasmodium* development remain elusive. Induction of mosquito

immune responses and bacteria-produced anti-*Plasmodium* factors have been implicated in this phenomenon²³.

The antimalarial activity of midgut microbiota provides the potential to convert mosquitoes into ineffective vectors^{21,24,25}. As part of this effort, we recently engineered the symbiotic bacterium Serratia AS1, which can spread into mosquito populations via vertical and horizontal transmission, to produce anti-Plasmodium effector molecules. The engineered bacteria effectively render mosquitoes resistant to Plasmodium infection²⁴. However, addressing the regulatory concerns of releasing genetically modified bacteria into the environment is a major challenge for the translation of these discoveries to the field. Identification of naturally occurring bacteria that can efficiently inhibit *Plasmodium* development and spread through mosquito populations would overcome this obstacle²⁶. Here we report the identification of *Serratia ureilytica* Su_YN1 from wild Anopheles sinensis mosquitoes in Tengchong, western Yunnan province (YN), that directly inhibits *Plasmodium* development via the secretion of a *Plasmodium*-killing lipase. Importantly, Su_YN1 can rapidly disseminate through mosquito populations.

Survey of the vector competence of the *A. sinensis* populations in China

While surveying the *Plasmodium vivax* malaria cases in different regions of China, we noticed that few local cases occurred in the city of Tengchong (YN; near the China–Myanmar border),

¹CAS Key Laboratory of Insect Developmental and Evolutionary Biology, CAS Center for Excellence in Molecular Plant Sciences, Shanghai Institute of Plant Physiology and Ecology, Chinese Academy of Sciences, Shanghai, China. ²CAS Center for Excellence in Biotic Interactions, University of Chinese Academy of Sciences, Beijing, China. ³The W. Harry Feinstone Department of Molecular Microbiology and Immunology and Johns Hopkins Malaria Research Institute, Bloomberg School of Public Health, Johns Hopkins University, Baltimore, MD, USA. ⁴Tengchong City Center for Disease Control and Prevention, Tengchong, China. ⁵National Health Commission Key Laboratory of Parasitic Disease Control and Prevention, Jiangsu Provincial Key Laboratory on Parasite and Vector Control Technology, Jiangsu Institute of Parasitic Diseases, Wuxi, China. ⁶National Institute of Parasitic Diseases, Chinese Center for Disease Control and Prevention, Shanghai, China. ⁷CAS Key Laboratory of Molecular Virology and Immunology, Institute Pasteur of Shanghai, Chinese Academy of Sciences, Shanghai, China. ⁸These authors contributed equally: Han Gao, Liang Bai. [™]e-mail: sbwang@cemps.ac.cn

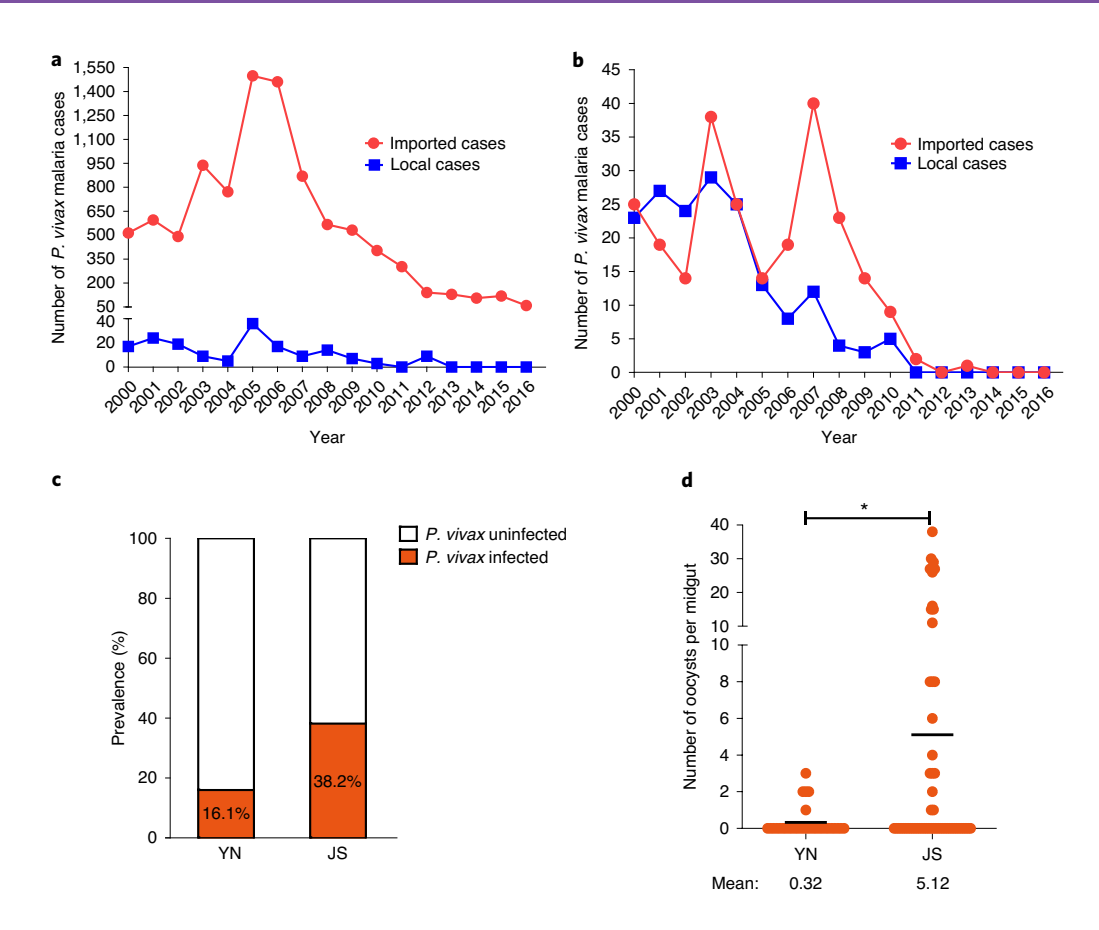


Fig. 1 | **Annual** P. vivax cases and A. sinensis susceptibility to P. vivax infection. a,b, Local and imported cases of P. vivax in YN (Tengchong; a) and JS (Wuxi; b) from 2000 to 2016. Statistical significance of the differences between the occurrence of local and imported cases were determined using two-tailed paired Student's t-tests. a, P < 0.0001; correlation coefficient of pairing (r) = 0.7314. b, P = 0.0852; r = 0.7192. c, Infection prevalence of wild-caught A. sinensis from YN and JS when fed P. vivax-infected blood. c0, Susceptibility of wild-caught C1. c0 sinensis mosquitoes from YN (r1) and JS (r1) to P1. c1 vivax infection. c2 vivax infection. c3 vivax infection. c4 vivax infection. c5 vivax infection individual midguts and the horizontal lines indicate the mean. Statistical significance between the two groups was determined using a two-tailed Mann-Whitney test; r2 = 0.0114; r3 < 0.05.

despite a high number of imported cases (Fig. 1a). In contrast, local malaria cases were highly correlated with imported cases in other regions such as the city of Wuxi (Jiangsu province (JS); Fig. 1b). Specifically, although the number of imported cases in YN was 500–1,450 annually before 2009, the number of local cases remained below 30 (Fig. 1a). Conversely, both imported and local cases in JS were frequent before 2009 (Fig. 1b), after which the number of cases sharply decreased at both locations, mainly

due to the implementation of the Chinese Government's 'Malaria Elimination Action' in 2010.

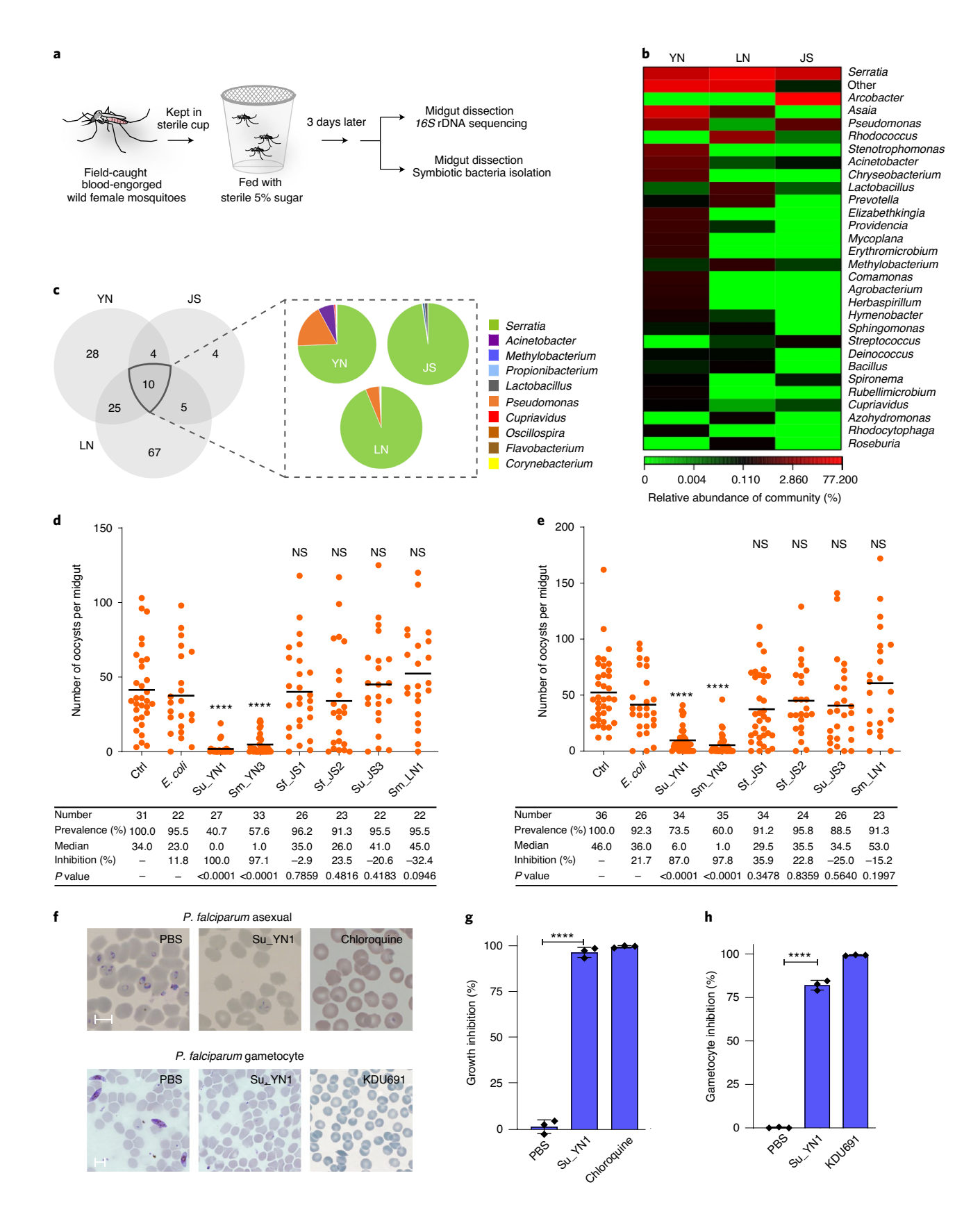
To test whether the difference in the rate of local transmission can be attributed to a difference in the susceptibility of *A. sinensis* to *P. vivax* infection, we fed *P. vivax*-infected patient blood to field-caught *A. sinensis* from YN and JS. The infection rate of the JS *A. sinensis* was 38.2%, which was more than double the percentage of infected YN *A. sinensis* (16.1%; Fig. 1c). Furthermore, the mean

Fig. 2 | Effect of gut symbiotic *Serratia* **bacteria of wild mosquitoes on** *Plasmodium* **development. a**, Workflow of the isolation and identification of mosquito-gut symbiotic bacteria using the gut symbiotic bacteria enrichment method. **b**, Heat map showing the relative abundance of the top 30 most abundant bacterial genera in *A. sinensis* mosquito populations from different geographical locations (YN, JS and LN; Supplementary Fig. 1). **c**, Composition and relative abundance of the genera shared between the three *A. sinensis* geographical populations. **d.e**, Effect of different *Serratia* strains on *P. falciparum* development in the midgut of *A. stephensi* (**d**) and *A. gambiae* (**e**) mosquitoes. Female mosquitoes were fed on 5% (wt/vol) sugar solution supplemented with PBS (Ctrl), *E. coli* or different *Serratia* strains. Su, *S. ureilytica*; Sm, *S. marcescens*; Sf, *S. fonticola*. The circles represent number of oocysts in individual midguts and the horizontal lines indicate the median. The sample size (number) of each group is listed in the tables (bottom). The experiments were repeated three times with similar results. Statistical significance of the differences in oocyst intensity between the *Serratia*-fed and *E. coli*-fed mosquitoes was determined using a two-tailed Mann-Whitney test. **f**, Images of Giemsa-stained parasites inhibited by the Su_YN1 culture supernatant (related to **g.h**). Scale bars, 5 μm. The experiments were repeated twice with similar results. **g**, Inhibition of *P. falciparum* growth (asexual) by the Su_YN1 culture supernatant. Chloroquine (5 μM) was used as a positive control. **h**, Inhibition of *P. falciparum* gametocyte formation by Su_YN1 bacteria in a trans-well assay. The *Plasmodium* Pl4K inhibitor KDU691 (20 μM) was used as a positive control. **g.h**, The experiments were repeated twice with similar results. Data are the mean ± s.d. The dots represent biologically independent replicates (*n* = 3). Statistical significant (*P* > 0.05).

number of oocysts in the midguts of JS mosquito (5.12) was higher than that of YN mosquitoes (0.32; Fig. 1d). These results suggest that *A. sinensis* mosquitoes from YN may be more resistant to *Plasmodium* infection than those from JS.

Serratia bacteria are the core gut symbionts of A. sinensis mosquitoes

The gut microbiome is a major determinant of mosquito vector competence²⁷. To explore the role of symbiotic bacteria of the gut



in modulating vector competence, we compared the composition of the gut symbiotic bacteria of *A. sinensis* from YN, JS and the city of Dandong (Liaoning province (LN)). The three geographical regions represent southwest, southeast and northeast parts of China (Supplementary Fig. 1). To isolate gut symbiotic bacteria, we first tested the persistence of two non-symbiotic bacteria—*Escherichia coli* and *Staphylococcus aureus*—in mosquito midguts. Both bacteria were completely egested one day after sugar feeding or three days after a blood meal (Extended Data Fig. 1), indicating that symbiotic bacteria can be enriched. We used this 'gut symbiotic bacteria enrichment method' (Fig. 2a) of maintaining field-caught blood-engorged mosquitoes in sterile cups and feeding them with sterile 5% sugar for three days to investigate the composition of symbiotic gut bacteria.

We extracted midgut DNA and conducted deep sequencing of 16S ribosomal DNA (rDNA) to examine the composition of the gut symbiotic bacteria. The bacterial composition differed between the three populations (Fig. 2b). A few taxa predominated in mosquitoes from the three locations and the proportions of the dominant genera also varied. *Asaia* (25.41%) and *Serratia* (16.21%) were the most abundant bacteria in the YN mosquitoes. *Serratia* (51.45%) and *Rhodococcus* (4.34%) were the most abundant in the LN mosquitoes. In the JS mosquitoes, *Arcobacter* (77.03%) and *Serratia* (21.11%) were the most abundant bacteria (Fig. 2b and Supplementary Tables 1–3).

Despite the differences in bacterial composition, the three mosquito populations shared ten bacteria genera—that is, *Serratia*, *Pseudomonas*, *Acinetobacter*, *Cupriavidus*, *Propionibacterium*, *Corynebacterium*, *Methylobacerium*, *Flavobacterium*, *Lactobacillus* and *Oscillospira* (Fig. 2c). Notably, the relative abundance of the genus *Serratia* was the highest among the shared gut bacterial symbionts in the three populations (Fig. 2c). Moreover, a retrospective analysis indicated that *Serratia* bacteria are the most widespread gut microbiota in *Anopheles* mosquitoes worldwide (Supplementary Fig. 2).

We also analysed the symbiotic bacteria of the mosquitoes using the culture method, and 128 distinct bacterial isolates were selected for *16S* rDNA sequence identification. The genera compositions were in good agreement with the deep sequencing results, with *Serratia* as the dominant core set of bacterial symbionts in *A. sinensis* (Supplementary Tables 1–3).

The genomes of the isolated Serratia strains were sequenced to further identify the bacterial species. Phylogenomic analysis revealed two species—S. ureilytica (Su_YN1) and Serratia marcescens (Sm_YN3)—in the YN A. sinensis populations, two species— Serratia fonticola (Sf_JS1) and S. ureilytica (Su_JS3)—in the JS A. sinensis populations and only S. marcescens (Sm_LN1) in the LN A. sinensis populations (Supplementary Fig. 3 and Supplementary Tables 1–3). Pathogenicity assays showed that none of these Serratia strains affected the survival of either A. sinensis or Anopheles stephensi (Extended Data Fig. 2a,b). To test Serratia colonization and persistence in the mosquito midgut, we integrated a green fluorescent protein gene (eGFP) into the chromosome of field Serratia strains. We found that these Serratia strains could stably colonize the female midgut, with an average of $1 \times 10^4 - 1 \times 10^5$ bacteria per sugar-fed midgut, and rapidly proliferated by more than 200-fold 24h after a blood meal (Extended Data Fig. 2c-e). These results confirm that our 'symbiont enrichment method' is effective.

YN Serratia bacteria impact Plasmodium development

We first used a rodent malaria model to investigate whether gut symbiotic bacteria affect vector competence. *Asaia, Acinetobacter* and *Pantoea* strains specific to YN had no detectable impact on *Plasmodium berghei* infection (Extended Data Fig. 3a). We next tested various symbiotic *Serratia* bacteria and found that two YN *Serratia* strains, Su_YN1 and Sm_YN3, strongly inhibited oocyst

formation (Extended Data Fig. 3b). We found that Su_YN1 and Sm_YN3 did not influence blood-feeding behaviour, fecundity or fertility (Extended Data Fig. 4a–c), thereby excluding the possibility that *Serratia* impacted *Plasmodium* development in mosquitoes by changing the mosquito biology.

We further investigated the effectiveness of the YN *Serratia* strains in inhibiting the development of the human malaria parasite *Plasmodium falciparum* in mosquitoes. *Serratia* Su_YN1 and Sm_YN3, but not the JS or LN *Serratia* strains, significantly inhibited oocyst formation in both *A. stephensi* (Fig. 2d) and *A. gambiae* (Fig. 2e) by up to 100% and 98%, respectively.

To examine whether the YN Serratia strains inhibit Plasmodium development via the activation of the mosquito immune system, we used RNA interference to silence the expression of Rel1 and Rel2, two NF-kB transcription factors that regulate the Toll and IMD immune-signalling pathways, respectively. Inhibition of the Toll pathway by Rel1 knockdown increased P. berghei infection of mosquitoes carrying Sm_YN3 compared with mosquitoes carrying Sm_ YN3 that were injected with double-stranded enhanced GFP RNA (dsGFP; Extended Data Fig. 5). However, silencing of the Toll or IMD pathway did not rescue parasite oocyst inhibition by Su YN1 (Extended Data Fig. 5). These results indicate that Sm_YN3 exerts its anti-*Plasmodium* activity by activation of the Toll immune pathway, whereas the mechanism of Su_YN1-mediated parasite inhibition is independent of modulation of these two mosquito immune pathways. This led us to further investigate the mechanism of Su YN1-mediated refractoriness.

Su_YN1 inhibits *Plasmodium* development through secretion of an antimalarial lipase

We next investigated whether *S. ureilytica* Su_YN1 inhibits parasite development before the oocyst stage. We found that ookinete formation is nearly totally inhibited by the Su_YN1 bacterial supernatant (Extended Data Fig. 6). These results indicated that Su_YN1 inhibits early stage parasite development in the mosquito gut by secretion of anti-*Plasmodium* factor(s).

The influence of gut bacteria on *Plasmodium* infection may be exerted through direct interactions with bacteria-produced anti-*Plasmodium* factors²³. We next investigated whether the culture supernatant of Su_YN1 can inhibit other stages of parasite development. We found that the Su_YN1 culture supernatant also strongly inhibits the development of *P. falciparum* asexual-stage parasites (Fig. 2f,g). Gametocyte development of *P. falciparum* was also inhibited when co-cultured with Su_YN1 bacteria in a trans-well system (Fig. 2f,h). Moreover, the Su_YN1 supernatant did not cause host red-blood-cell lysis (Extended Data Fig. 7), indicating a direct inhibitory effect on the parasite.

We used solvents of varying polarity to extract compounds from the Su_YN1 culture supernatant to investigate whether the antimalarial factor is a metabolite, but none of the extracts had antimalarial activity (Extended Data Fig. 8a). However, trypsin digestion of the Su_YN1 culture supernatant completely abolished its antimalarial activity (Extended Data Fig. 8b), indicating that the antimalarial factor may be either a peptide or a protein. We then separated the culture supernatant using a centrifugal filter with a 3-kDa cutoff and tested the antimalarial activity of the retentate and filtrate. Only the retentate showed strong antimalarial activity (Extended Data Fig. 8c), indicating that the antimalarial factor may be a secreted protein.

To identify the antimalarial protein in Su_YN1, we selected two strains of *S. ureilytica* with different anti-*Plasmodium* activities for further analysis. Su_YN1 has strong antimalarial activity but Su_JS3 has no antimalarial activity. The Su_YN1 and Su_JS3 supernatant proteins were subjected to SDS-polyacrylamide gel electrophoresis (SDS-PAGE) and identified by mass spectrometry. The differentially expressed proteins with higher abundance were selected

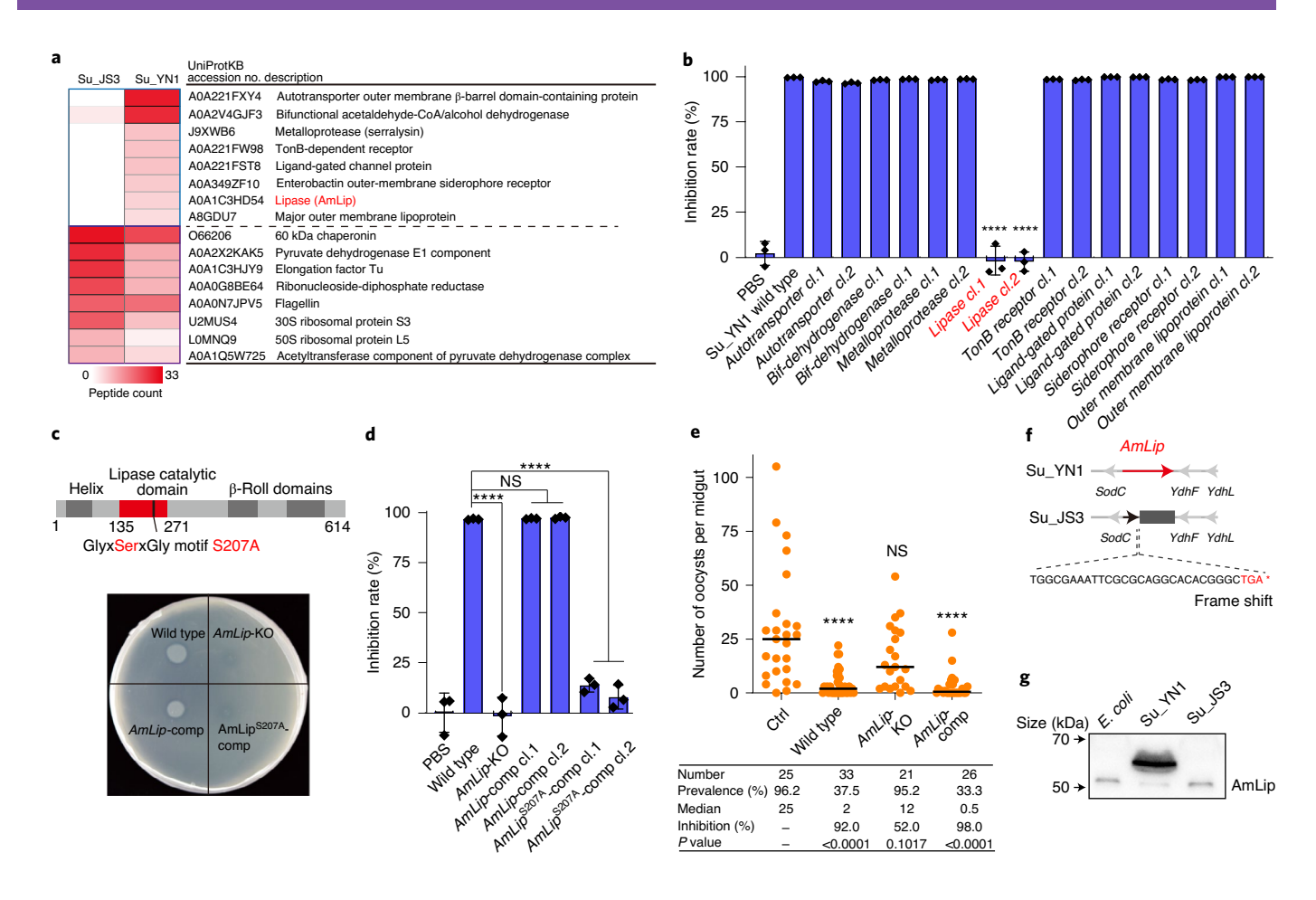


Fig. 3 | Identification of the secreted antimalarial lipase AmLip in S. ureilytica Su_YN1. a, Comparative analysis of the proteins secreted by the antimalarial S. ureilytica strain Su_YN1 and non-antimalarial S. ureilytica strain Su_JS3. The proteins with higher abundance that were differentially expressed by Su_YN1 and Su_JS3 are displayed; AmLip is highlighted in red font. **b**, Lipase AmLip is responsible for the antimalarial activity of Su_YN1. The genes coding for the proteins in a were knocked out in Su_YN1 and the culture supernatants of the mutants were used in in vitro ookinete inhibition assays. Two clones of each mutant were tested. Data are the mean \pm s.d. The dots represent biologically independent replicates (n=3). Statistical significance of the test inhibition rate compared with the Su_YN1 wild-type group was determined using a two-tailed Student's t-test. c, Measurement of lipase enzymatic activity using the lipoprotein plate degradation assay (bottom). Culture supernatants (10 µl) of the indicated bacterial Su_YN1 strains were spotted on an egg yolk plate and incubated for 20 h at 30 °C. Lipase activity was visualized by the lytic spot. The S207A mutation abolished lipase activity. The lipase protein structure is shown with the amino-acid-residue positions indicated (top). d, In vitro Plasmodium yoelii ookinete inhibition assay of the culture supernatants of the indicated Su_YN1 strains. Data are the mean \pm s.d. The dots represent biologically independent replicates (n=3). The experiments were repeated three times with similar results. Statistical significance of the test inhibition rate compared with the wild-type group was determined using a two-tailed Student's t-test; the P values were as follows: <0.0001 (AmLip-KO, AmLip^{5207A}-comp cl.1) and AmLip^{5207A}-comp cl.2), 0.2224 (AmLip-comp cl.1) and 0.0759 (AmLip-comp cl.2). e, P. berghei ANKA oocyst load in A. stephensi mosquitoes fed with the indicated Su_YN1 strains. The circles represent the number of oocysts in individual midguts and horizontal lines indicate the median. The sample size (number) of each group is listed in the table (bottom). The experiments were repeated twice with similar results. Statistical significance of the difference in oocyst intensity compared with the control group was determined using a two-tailed Mann-Whitney test. c-e, AmLip-comp, AmLip complemented strain; AmLip^{S207A}-comp, AmLip^{S207A} point-mutant complemented strain: f, Diagram showing a premature termination codon (indicated in red) in the AmLip coding region of Su JS3, leading to early termination of translation, g. Western blot detection of AmLip protein in the Su_YN1 and Su_JS3 culture supernatants using anti-AmLip antiserum. The experiments were repeated twice with similar results. ****P < 0.0001; NS, not significant (P > 0.05).

(Fig. 3a) and each of the Su_YN1-enriched genes were knocked out. Of these, only deletion of the lipase gene (*COG2931*) abolished antimalarial activity (Fig. 3b). We named this 65-kDa lipase Antimalaria Lipase (AmLip). Sequence analysis revealed that AmLip belongs to the I.3 lipase family (E.C.3.1.1.3) with a conserved pentapeptide Gly-X-Ser-X-Gly motif^{28,29} (Fig. 3c and Supplementary Fig. 4). A lipase-activity assay using the trioleoylglycerol-rhodamine B-specific plate assay confirmed the lipase activity of AmLip (Supplementary Fig. 5). AmLip could also hydrolyze complex lipids, as indicated by the egg yolk plate assay (Fig. 3c). The S207A

mutation in the Gly-X-Ser-X-Gly motif completely abolished the hydrolytic activity (Fig. 3c). Moreover, two complemented strains (AmLip-comp cl.1 and cl.2) could rescue the antimalarial activity of the mutant, whereas complementation by the S207A mutant did not (Fig. 3d). These results indicate that Su_YN1 inhibits *Plasmodium* by the secretion of AmLip.

To investigate whether AmLip expression contributes to the antimalarial activity of *Serratia* Su_YN1 in the mosquito midgut, we fed *A. stephensi* mosquitoes with sugar meals containing living wild-type Su_YN1, its *AmLip*-knockout (*AmLip*-KO) mutant

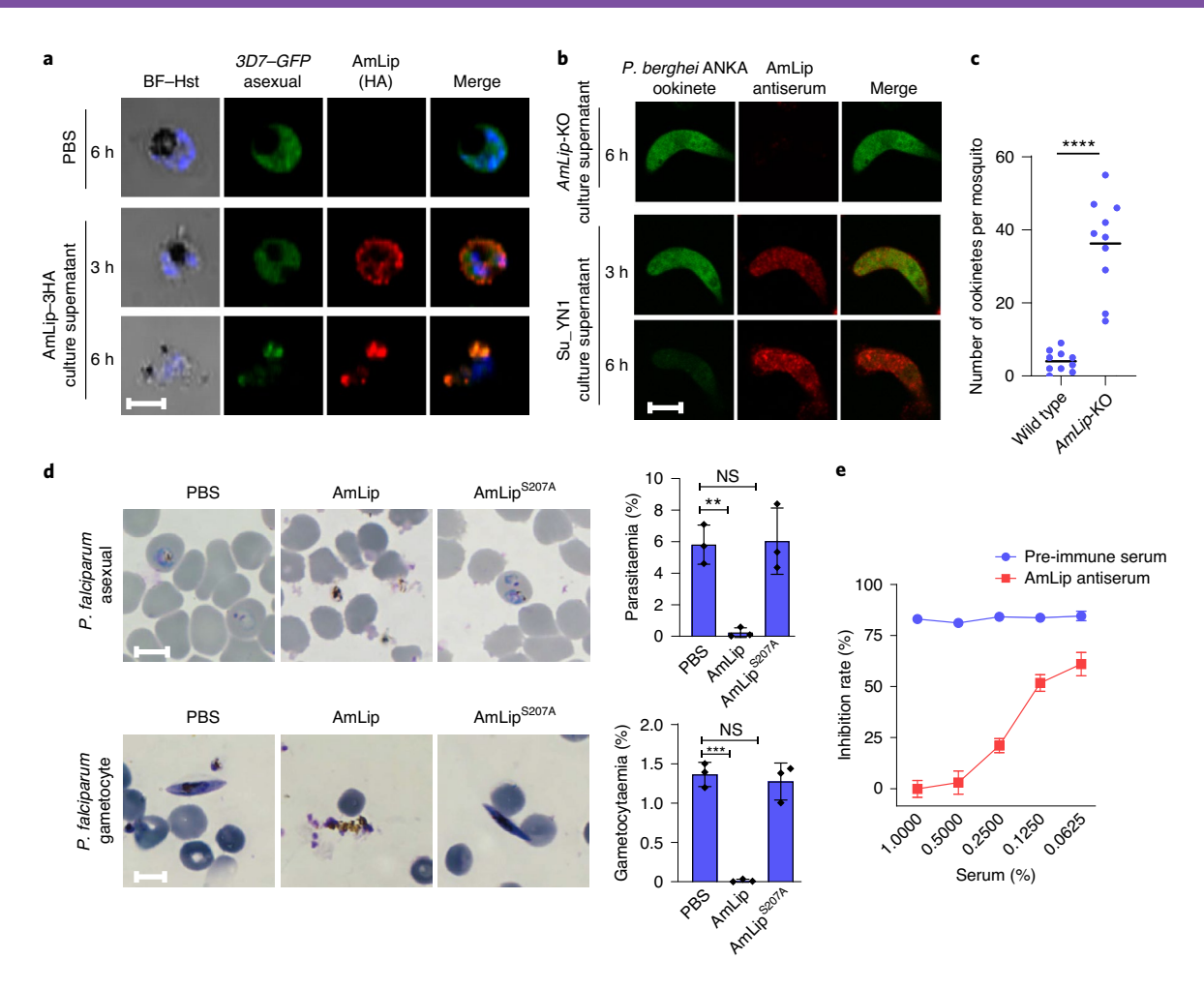


Fig. 4 | AmLip disrupts and kills parasites. a, Indirect immunofluorescence detection of AmLip in P. falciparum 3D7 asexual parasites. The 3D7-GFP parasites were incubated with the culture supernatant of 3HA-tagged AmLip (Extended Data Fig. 10a). Binding of AmLip protein to the parasite was detected using HA antibody. The experiments were repeated twice with similar results. BF-Hst, Bright-field images of Hoechst 33342 staining. b, Indirect immunofluorescence detection of AmLip in P. berghei ANKA ookinetes. GFP-labelled ookinetes were incubated with the culture supernatant from wild-type Su YN1 (bottom) and the AmLip-KO mutant (top). Binding of AmLip protein to the ookinete was detected using AmLip mouse antiserum. The experiments were repeated twice with similar results. c, P. falciparum ookinete load in A. stephensi carrying wild-type Su YN1 or its AmLip-KO mutant strain. The mosquitoes (n = 10 mosquitoes per group) were fed mature P. falciparum gametocytes, their midguts were dissected 20 h post feeding and the ookinetes in the bolus were counted. The circles represent the number of ookinetes in individual midguts and horizontal lines indicate the median. This experiment was repeated twice with similar results. Statistical significance was analysed using a two-tailed Mann-Whitney test. d, AmLip disrupts the growth and gametocytaemia of P. falciparum parasites. Purified AmLip and AmLip^{5207A} protein were added to P. falciparum 3D7 asexual (top) and gametocyte (bottom) cultures at a final concentration of $5 \mu g \, ml^{-1}$ and incubated for 24 h. The parasites were observed using Giemsa staining (left) and the per cent inhibition was calculated relative to the PBS controls (right). The experiments were repeated twice with similar results. Data are the mean ± s.d. The dots represent biologically independent replicates (n=3). Statistical significance of the test inhibition rate compared with the PBS control was determined using a two-tailed Student's t-test. Top: P = 0.0016 (AmLip) and 0.8817 (AmLip^{5207A}); bottom: P = 0.0001 (AmLip) and 0.6151 (AmLip^{5207A}). e, AmLip antiserum neutralizes the antimalarial activity of the Su_YN1 culture supernatant. Various amounts of AmLip antiserum were added to an ookinete culture. Pre-immune serum was used as a negative control. Data are the mean \pm s.d. The dots represent biologically independent replicates (n=3). Scale bars, $5 \mu m. ****P < 0.0001; ***P < 0.001; **P < 0.01; NS, not significant (P > 0.05).$

and the complemented strains. As expected, *AmLip* knockout compromised the antimalarial activity, whereas complementation of *AmLip* restored antimalarial activity (Fig. 3e). We next compared the *AmLip* expression of the field-isolated *Serratia* strains. *AmLip* transcript was only detected in two *S. ureilytica* strains (Su_YN1 and Su_JS3) and was undetectable or present at very low levels in the other *Serratia* strains as well as *E. coli* (Extended Data Fig. 9). However, AmLip protein was not detected in the mass-spectrometry analysis of Su_JS3 (Fig. 3a). Analysis of the Su_JS3 *AmLip* gene sequence revealed a frame shift that leads to early termination of translation and synthesis of a truncated

non-functional protein (Fig. 3f). This was confirmed by western blotting (Fig. 3g).

AmLip directly targets and kills *Plasmodium* parasites

To investigate how AmLip inhibits the malaria parasite, we expressed AmLip-haemagglutinin (HA) fusion protein in Su_YN1 (Extended Data Fig. 10a). Immunofluorescence assays revealed that HA-tagged AmLip signal could be detected on *P. falciparum* parasites in the asexual stage after incubation with AmLip-HA-expressing culture supernatant (Fig. 4a). To further investigate the interaction between AmLip and parasites, rodent malaria ookinetes were incubated

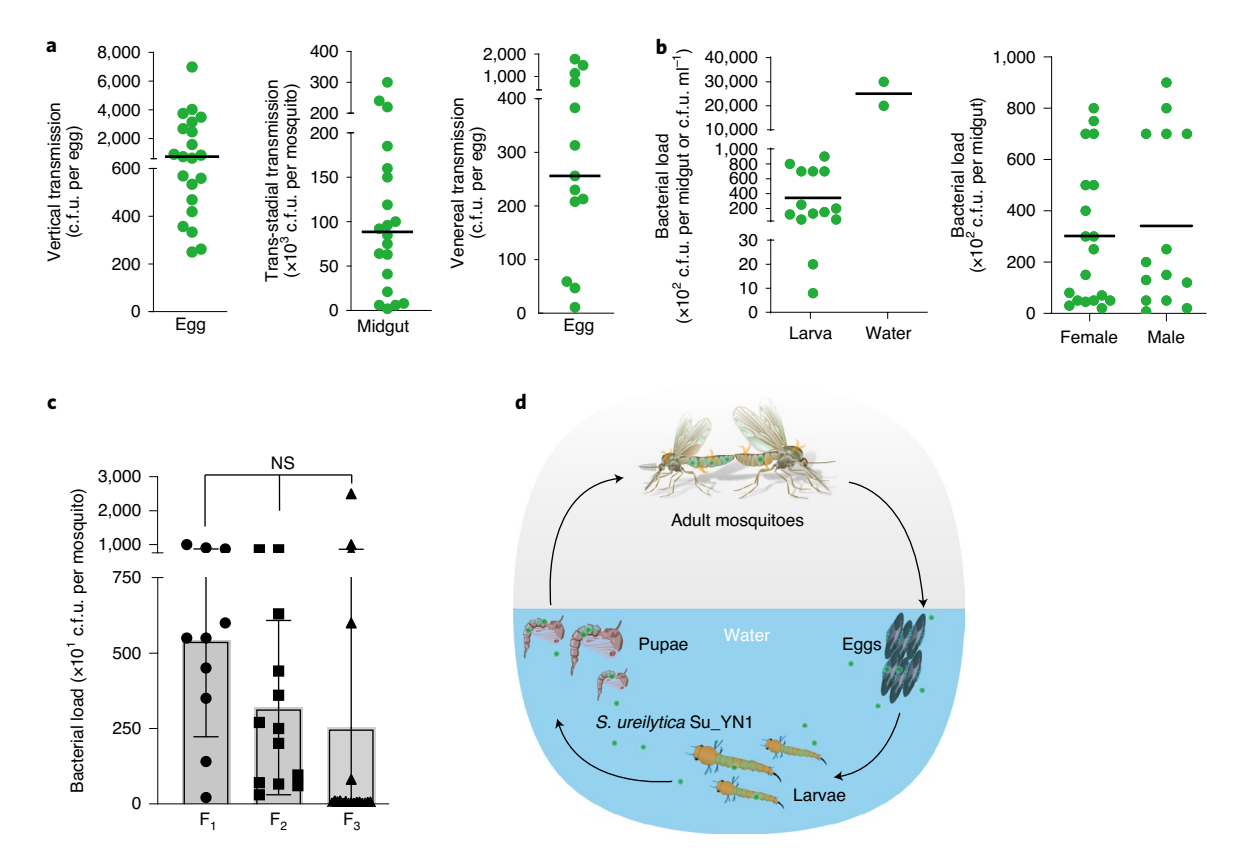


Fig. 5 | *S. ureilytica* **Su_YN1** bacteria spread efficiently through mosquito populations. **a**, Su_YN1 is transmitted vertically via laid eggs (n=21; left), trans-stadially from larvae to adult mosquitoes (n=20; middle) and venereally from male to female mosquitoes (n=13; right). The circles represent the number of colony-forming units (c.f.u.) in individual eggs or midguts and horizontal lines indicate the median number of Su_YN1 per egg or midgut. The experiment was repeated three times with similar results. **b**, Bacterial load in larva (c.f.u. per midgut; n=14) and breeding water (c.f.u. ml⁻¹) (left) as well as in adult midguts (right; female (n=20) and male (n=14)). **c**, Su_YN1 was transmitted for three consecutive generations. Ten male mosquitoes fed with fluorescent *S. ureilytica* Su_YN1 bacteria were introduced into a cage with 190 non-bacteria-fed males and 200 virgin females (Supplementary Fig. 7), allowed to mate and the eggs were collected and reared to adults to yield generation F_1 . Eggs from these adults were reared without further addition of Su_YN1 bacteria to yield F_2 . F_3 was generated similarly. The number of Su_YN1 bacteria in adult female mosquitoes of F_1 (n=10), F_2 (n=13) and F_3 (n=20) were determined. Data are presented as the mean \pm s.d. Statistical significance was determined using a one-way ANOVA (without matching or pairing) analysis of variance; P=0.2887; NS, not significant (P>0.05). **d**, Diagram illustrating how Su_YN1 originating from males can spread efficiently through a subsequent mosquito population and be maintained through a complete mosquito life cycle.

with the supernatant of wild-type Su_YN1 and its *AmLip*-deletion mutant. AmLip signal was detected by immunofluorescence using an AmLip antiserum (Extended Data Fig. 10b). An AmLip signal could be detected on ookinetes that were incubated with the supernatant of wild-type Su_YN1 but not the mutant strain (Fig. 4b). The AmLip protein gradually accumulated on the parasites and eventually led to parasite death, as indicated by loss of GFP signal (Fig. 4a,b). To examine the killing effect of AmLip protein on *P. falciparum* ookinetes in vivo, *A. stephensi* mosquitoes carrying wild-type or *AmLip*-KO mutant Su_YN1 bacteria were fed mature *P. falciparum* gametocytes. As expected, wild-type Su_YN1 strongly inhibited *P. falciparum* ookinete formation in the gut lumen of *A. stephensi* compared with the *AmLip*-KO mutant (Fig. 4c).

To further confirm the direct killing effect of AmLip, we produced a recombinant AmLip protein by expressing it in *E. coli* DE3 (Extended Data Fig. 10c). Lipase activity of the purified AmLip protein was confirmed with a lipoprotein plate degradation assay (Extended Data Fig. 10d,e). The AmLip^{S207A} mutant protein that lost lipase activity was also prepared (Supplementary Fig. 6). Addition of purified AmLip protein, but not AmLip^{S207A} mutant protein, led to death of *P. falciparum* asexual and gametocyte parasites (Fig. 4d). Moreover, an AmLip antiserum blocked the AmLip malaria-killing effect in a dose-dependent manner (Fig. 4e). These results show

that AmLip directly targets and kills *Plasmodium* parasites via its lipase activity.

Su_YN1 disseminates efficiently into mosquito populations

We next examined whether Su_YN1 bacteria can be transmitted by mosquitoes. We found that Su_YN1 is transmitted at three different stages: (1) vertical transmission from females to progeny by attaching to the egg surface, (2) trans-stadial transmission from larvae to adults and (3) sexual transmission from males to females (Fig. 5a). These properties suggested that Su_YN1 can spread through mosquito populations. To test this hypothesis, we conducted a cage experiment in which a small number (5%) of male mosquitoes that had previously fed on eGFP-tagged Su_YN1 were introduced into a cage containing virgin male and females that did not have Su_YN1 (Supplementary Fig. 7). These mosquitoes were fed blood, and the eggs were collected and raised to the adult stage. A high titre of Su_YN1 bacteria was detected in the breeding water, indicating that Su_YN1 propagated in the water and were ingested by the larvae (Fig. 5b). Moreover, 100% of the adult progeny carried Su_YN1 (Fig. 5b and Supplementary Fig. 7). Importantly, Su_YN1 was transmitted for three consecutive generations (Fig. 5c), indicating that Su_YN1 has stable symbiosis with mosquitoes and can effectively spread through mosquito populations (Fig. 5d).

Discussion

In this study we showed that *A. sinensis* mosquito populations in YN are more resistant to infection with *P. vivax* and that the composition of the gut microbiota plays a crucial role in determining mosquito resistance to *Plasmodium* infection.

The mosquito-gut microbiota is highly dynamic and varies greatly between individual mosquitoes³⁰, as opportunistic bacteria ingested from different sources may transiently colonize the midgut. Previous studies showed that some bacteria isolated from sugar-fed mosquitoes cannot stably colonize the mosquito midgut¹². Ingestion of a blood meal affects the bacterial colonization dynamics and shapes the composition of the midgut microbiota³¹. The transient bacteria are usually cleared in less than two days after blood ingestion³². Moreover, the bacterial load in the mosquito midgut undergoes dramatic proliferation, peaking at around 24-30h after a blood meal^{21,33}, when malaria parasites suffer dramatic losses during their development in mosquitoes¹³. In this context, understanding of the composition of the midgut microbiota at the time of parasite infection is important. In this study we showed that non-symbiotic bacteria are egested two days after a blood ingestion, and this served as a basis to develop a gut symbiotic bacteria enrichment method. Different populations of A. sinensis share a core set of symbiotic bacteria, Serratia being the dominant genus among field-collected Anopheles mosquitoes worldwide34-36, which suggests that Anopheline mosquitoes retain microbiota in a selective way.

Our findings show that different species of *Serratia* and different strains of the same species of *S. ureilytica* have different effects on *Plasmodium* development, demonstrating that the effect of mosquito-gut symbionts on parasite infection depends on species-specific or strain-specific interactions, in accordance with previous reports^{25,37}. Our results underscore the fact that symbiotic bacteria can modulate parasite infection via different mechanisms.

Serratia bacteria secrete a broad range of proteins, such as haemolysin and serralysin³⁸. Lipids are a major component of parasite membranes³⁹. Our study showed that Su_YN1 secretes the AmLip enzyme that kills malaria parasites. Family I.3 lipases, secreted through the type I secretion system, are lipolytic enzymes that catalyse the hydrolysis of ester bonds. By generating a point mutant of the conserved active site, we showed that lipid hydrolysis is critical for the antimalarial activity of AmLip. Interestingly, AmLip can disrupt asexual parasites without lysing the red blood cell, suggesting that AmLip selectively targets the parasite.

Serratia bacteria are dominant gut symbionts of anopheline mosquitoes and are commonly present in water, soil and plant surfaces^{17,23,24}. S. ureilytica Su_YN1 can colonize different malaria-vector mosquitoes and through efficient vertical and horizontal transmission, it can spread rapidly through mosquito populations while rendering mosquitoes resistant to human malaria infection. Introduction of S. ureilytica Su_YN1 into wild populations may plausibly be implemented by addition to mosquito breeding water and/or via sugar baits, thereby providing a powerful tool for malaria control.

Methods

Ethics statement. This study was carried out in accordance with the guidelines of the CAS Center for Excellence in Molecular Plant Sciences (Shanghai Institute of Plant Physiology and Ecology) Animal Care and Use Committee (A01MP2001) and the guidelines of the Johns Hopkins University Animal Care and Use Committee (M018H18). *P. vivax* infectious blood was collected from patients who provided written informed consent, and was approved by the National Institute of Parasitic Diseases Ethics Committee (2015-010).

Mosquito rearing. Both *A. stephensi* (Dutch strain) and *A. gambiae* (Keele strain) mosquitoes were maintained on 10% sugar solution at $27\,^{\circ}$ C and $70\pm5\%$ relative humidity (RH) under a 12h light–12h dark cycle. Larvae were fed on cat food pellets and ground fish food supplement.

Susceptibility of wild-caught *A. sinensis* mosquitoes to *P. vivax* infection. *P. vivax* blood samples were collected from patients older than 18 yrs. Thick

and thin blood smears were air dried, fixed with methanol and stained with 10% Giemsa solution for 10 min. The gametocyte densities were calculated by counting the number of parasites per 500 leukocytes in a thick blood smear under oil-immersion microscopy. The counts were then converted to gametocytes μl^{-1} by assuming a count of 8,000 leukocytes μl^{-1} blood with 500–2,000 *P. vivax* gametocytes μl^{-1} was used to infect *A. sinensis* mosquitoes. Infectious blood (500 μ l) was centrifuged at 5,000 g for 5 min and the serum was replaced with 300 μ l naive AB serum to avoid interference from patient factors.

Blood-engorged wild female mosquitoes were collected from house walls using a mouth aspirator and maintained at $26\pm2\,^{\circ}\mathrm{C}$ and $70\pm5\%$ RH. After three days, these mosquitoes were allowed to lay eggs. The resulting larvae were fed on cat food pellets and ground fish food supplement, and reared to adulthood following standard protocol. The female adults that emerged from these eggs (4–6 days old) were fed on *P. vivax*-infected blood using a membrane feeder as described**0. The engorged mosquitoes were maintained in an incubator at $26\,^{\circ}\mathrm{C}$ and $70\pm5\%$ RH. Eight days after the infective blood meal, mosquito midguts were dissected in $1\times\mathrm{PBS}$, stained with 0.2% mercurochrome and examined for oocyst load.

Colonization persistence of non-symbiotic bacteria in *Anopheles* midguts. GFP-labelled *E. coli* and mCherry-labelled *S. aureus* were used for non-symbiotic bacteria sustainability in the midguts of *A. stephensi* and *A. sinensis*. After culturing in Luria–Bertani (LB) medium at 37 °C overnight, the bacteria were washed with sterile 1×PBS and resuspended to a final concentration of $1\times10^\circ$ c.f.u. ml $^{-1}$. After a 10-h starvation, female mosquitoes were fed for 48 h on 5% sugar containing bacteria ($1\times10^\circ$ c.f.u. ml $^{-1}$). The mosquitoes were surface-sterilized with cold 75% ethanol for 3 min and washed three times with sterile PBS. Their midguts were dissected under sterile conditions at different time points before and after a blood meal and homogenized in sterile PBS. The bacterial load was determined by plating tenfold serial dilutions of the homogenates on LB agar plates (10 g l $^{-1}$ tryptone, 5 g l $^{-1}$ yeast extract, 5 g l $^{-1}$ sodium chloride, 10 g l $^{-1}$ agar, pH7.2) containing 50 µg ml $^{-1}$ kanamycin and incubating at 30 °C for 24 h. Fluorescent colonies were counted by fluorescence microscopy.

Isolation of gut symbiotic bacteria from field-caught A. sinensis.

Blood-engorged field-caught female A. sinensis mosquitoes were collected in three different regions of China—Tengchong in YN, Wuxi in JS and Dandong in LN (Supplementary Fig. 1). The mosquitoes were collected from house walls using a mouth aspirator and reared in sterilized cups maintained at 26 ± 2 °C and 70 ± 5 % RH. To allow for the egestion of non-symbiotic bacteria and enrichment of symbiotic bacteria, the field-caught blood-engorged mosquitoes were kept in sterile cups and fed with sterile 5% sugar, which was replaced every 12h, for 3 d. These mosquitoes were then surface-sterilized with 75% ethanol and washed three times with sterile 1×PBS. Their midguts were dissected under sterile conditions. The midguts of 20 female A. sinensis were used to isolate symbiotic bacteria. Five serials of tenfold dilutions of the gut homogenates were spread on LB agar plates. The plates were incubated at 28 °C for 24 h. The bacterial colonies were classified based on morphological parameters (shape, colour and colony size). Genera of the various representative colonies were further identified by 16S rDNA sequencing.

DNA extraction and 16S rDNA amplicon deep sequencing. Mosquitoes were surface-sterilized with cold 75% ethanol for 3 min and washed three times with sterile 1×PBS. Each group had two replicates, and 40-50 mosquitoes from two replicates were mixed to obtain enough samples. The bacterial DNA was purified using the Gentra puregene yeast/bact. kit B (Qiagen). The V3-V4 hypervariable region of the 16S rDNA was amplified using the forward primer 343F (5'-TACGGRAGGCAGCAG-3') and the reverse primer 798R (5'-AGGGTATCTAATCCT-3'). Sequencing of the 16S amplicon was performed by OE Biotech Co., Ltd. on an Illumina MiSeq with two paired-end read cycles of 300 bases each. Paired-end reads were pre-processed using Trimmomatic41 to cut off low-quality sequences and assembled using FLASH42. Reads with 75% of the bases above Q20 were retained using QIIME (version 1.8.0)43. Clean reads were used to generate operational taxonomic units using VSEARCH with a 97% similarity cutoff14. A representative read of each operational taxonomic unit was selected using the QIIME package, annotated and blasted against the Silva database (version 123) using RDP classifier (the confidence threshold was 70%)⁴⁵.

16S rDNA cloning and sequencing for bacterial identification. The 16S rDNA of the isolated bacterial DNA was PCR amplified using the primers 27F (5'-AGAGTTTGATCMTGGCTCAG-3') and 1492R (5'-GGTTACCTTGTTACGACTT-3'), which produced a fragment of approximately 1.5 kb. The PCR products were purified using a Cycle pure kit (OMEGA) and sequenced using an ABI Prism 3730 sequencer (Applied Biosystems). The 16S rDNA sequences were aligned with the closest relatives found in the GenBank database by a BLAST search. The phylogenetic tree was constructed using the neighbour-joining method with the MEGA7 software 46.

Whole-genome sequencing and de novo assembly of *Serratia* bacteria. A paired-end DNA library with an insert size of 500 bp was constructed and sequencing reactions were performed by OE Biotech Co., Ltd. on an Illumina MiSeq PE300 platform. The low-quality reads were filtered by the SMRT 2.3.0

software⁴⁷ and the filtered reads were assembled by SOAP de novo (http://soap.genomics.org.cn) to generate scaffolds.

Phylogenomic analysis. Construction of the orthologue groups of proteins was performed using OrthoMCL v2.0 (http://orthomcl.org/orthomcl/)⁴⁸. The genome-sequence accession numbers of the bacteria can be found in Supplementary Fig. 3. Amino-acid sequences of the single-copy orthologous proteins were aligned using MUSCLE using the default parameters⁴⁹. Non-conserved regions in each multiple alignment were removed using trimAl (http://trimal.cgenomics.org/)⁵⁰. A maximum-likelihood phylogenomic tree was created using 1,000 full-bootstrap replicates using PhyML⁵¹ and the best model (Whelan and Goldman; WAG) identified by ProtTest⁵².

Generation of GFP-tagged Serratia bacteria strains. To integrate the eGFP gene into the chromosome of Serratia strains, the transposon plasmid pBAM2-GFP²4 was individually transformed into a donor strain E. coli S17–1 λ pir. The freshly cultured pBAM2-GFP-harbouring donor strain and recipient Serratia strain cells were separately washed and resuspended in 10 mM MgSO4 solution (OD600 of 0.1 for each strain), mixed (1:1) and co-cultured on LB agar plates at 37 °C for 5 h for conjugation mating.

Colonization and quantification of bacteria in the mosquito midgut.

GFP-tagged Serratia bacteria were cultured overnight in LB broth at 28 °C. The bacteria were harvested by centrifugation at 3,000g for 10 min, washed three times in sterile PBS and resuspended in 5% sterile sucrose solution to obtain 1×10^7 cells ml $^{-1}$. These bacteria were administered to two-day-old female mosquitoes for 36 h using soaked cotton pads, after which the bacteria-containing cotton pads were replaced with sterile cotton pads moistened with 10% sucrose solution. Two days later, the mosquitoes were fed on a blood meal, surface-sterilized with cold 75% ethanol, and their midguts were dissected under sterile conditions 1, 3, 7 and 14 days post the blood meal and homogenized in sterile PBS. The bacterial numbers were determined by plating tenfold serial dilutions of the homogenates on LB agar plates supplemented with 50 μ g ml $^{-1}$ kanamycin and incubating at 30 °C for 24 h. Fluorescent colonies were counted by fluorescence microscopy.

Effect of Serratia bacteria on the mosquito lifespan. Serratia bacteria were administered to two-day-old adult A. sinensis and A. stephensi for 36 h via a 5% sugar meal with $(1\times10^7\,{\rm cells\,ml^{-1}})$ or without bacteria (control). Two days later, the mosquitoes were fed on an uninfected mouse. The mosquito survival was monitored daily.

Effect of Serratia bacteria on mosquito blood feeding, fecundity and fertility. Serratia bacteria were cultured overnight in LB medium, washed three times in sterile 1×PBS and fed to two-day-old female mosquitoes for 36 h using a cotton pad soaked with a 5% sucrose solution with $(1\times10^7\,{\rm cells\,ml^{-1}})$ or without (PBS) bacteria. Two days later, the mosquitoes were fed on a healthy mouse. The numbers of engorged and non-engorged mosquitoes were counted. Individual female mosquitoes were allowed to lay eggs on a damp filter paper in an oviposition tube two days post a blood meal. Females that laid eggs were carefully removed from the tubes. After three days, the number of eggs were counted and classified as intact (unhatched) or broken (hatched).

Effect of bacteria on *P. berghei* infection in mosquitoes. Bacteria were cultured overnight in LB medium and washed three times with sterile $1\times PBS$. Axenic female mosquitoes were generated via oral antibiotics as described previously ⁵³. Aseptic mosquitoes were fed for 36 h on a cotton pad soaked with a 5% sucrose solution with $(1\times 10^7\, \text{cells ml}^{-1})$ or without bacteria (PBS), and then fed on a *P. berghei*-infected mouse and maintained at $19\,^{\circ}C$ and 80% RH. Mosquitoes that had not fed were removed and the fully engorged mosquitoes were provided with 5% (wt/vol) sterile sucrose solution. Their midguts were dissected on day 12 after the blood meal and stained with 0.1% (wt/vol) mercurochrome to determine the oocyst load.

Effect of bacteria on *Plasmodium falciparum* infection. Serratia bacteria were administered to axenic female A. stephensi and A. gambiae for 36 h via a cotton pad soaked with a 5% sucrose solution with $(1\times10^7\,{\rm cells\,ml^{-1}})$ or without (PBS) bacteria and the mosquitoes were then allowed to feed on P. falciparum NF54 gametocyte-containing blood, as described previously²¹. The engorged mosquitoes were kept in an incubator at 26 °C and 80% RH. Their midguts were dissected in 1xPBS eight days post infection, stained with 0.1% mercurochrome and the oocysts were counted.

RNA extraction from mosquito midguts. The mosquito midguts were dissected in ice-cold PBS and stored in 200 μl RNAiso plus. Total RNA was extracted accorded to the RNAiso plus (Takara) protocol, followed by RNase-free DNase I (Thermo Scientific) treatment.

Quantitative real-time PCR analysis. Complementary DNA was synthesized from total RNA using a PrimeScript RT reagent kit with gDNA Eraser (Takara)

according to the manufacturer's instructions. Quantitative real-time PCR analysis was performed using a PikoReal 96 (Thermo) and the AceQ qPCR SYBR Green master mix (Vazyme). The primers are shown in Supplementary Table 4.

Double-stranded RNA synthesis and gene silencing in adult mosquitoes. To produce $\it Rel1$ and $\it Rel2$ double-stranded RNA (dsRNA), the coding regions were PCR-amplified from $\it A$. $\it stephensi$ cDNA with forward and reverse primers containing a T7 promoter sequence at their 5' end (5'-TAATACGACTCACTATAGGG-3'). The primer sequences are listed in Supplementary Table 4. The PCR products were purified using a Cycle pure kit (OMEGA) and used to synthesize dsRNA in vitro using a MEGAscript RNAi kit (Life Technologies). The dsRNA was purified and concentrated to $3\,\mu g\,\mu l^{-1}$ using a Microcon YM-100 filter (Millipore); dsGFP was synthesized as a negative control. To conduct RNA interference-mediated gene silencing, three- or four-day-old female mosquitoes were intrathoracically injected with 69 nl dsRNA solution using a Nanoject II microinjector (Drummond). The control mosquitoes were injected with dsGFP. The injected mosquitoes were allowed to recover for 2–3 days before conducting parasite infection.

Preparation of bacterial culture supernatant for the anti-*Plasmodium* activity assay. Bacteria were cultured overnight at 30 °C in RPMI 1640 medium containing 10% fetal bovine serum. The bacterial cultures were centrifuged under 3,000g for 20 min, and the supernatants were filtered through a 0.22-µm filter to remove bacterial cells and used for the antimalarial activity assay.

In vitro anti-Plasmodium activity assays of asexual-stage P. falciparum.

Synchronous ring-stage P. falciparum was generated using 5% sorbitol. Filtered bacterial supernatant ($10\,\mu$ l) was added to three wells of 96-well plates, followed by the addition of $190\,\mu$ l of synchronous ring-stage P. falciparum cultures at 1% haematocrit and 1% parasitaemia. The positive control was chloroquine and the negative control was the parasite growth medium. After 72 h of incubation at 37 °C, $100\,\mu$ l supernatant was removed and $100\,\mu$ l SYBR green-I solution with lysis buffer ($20\,\mathrm{mM}$ Tris, pH7.5, 5 mM EDTA, 0.008% (wt/vol) saponin and 0.08% (vol/vol) Triton X-100) was added to each well. The plates were then incubated for $2\,\mathrm{h}$ in the dark at room temperature. All of the plates were read using a fluorescence plate reader, with excitation and emission wavelengths of 485 and 535 nm, respectively. The inhibition rate was calculated relative to the parasite-growth-medium negative control (0% inhibition). Three biological replicates were assayed.

In vitro anti-Plasmodium activity assays of ookinete-stage P. berghei. To assess the inhibition of P. berghei ookinete formation, female ICR mice (7 weeks old) were infected with P. berghei. Three days post infection, blood with high gametocytaemia was collected by heart puncture and used for in vitro ookinete culture as described previously⁵⁴. To assess the inhibition of ookinete development of P. yoelii parasites, a transgenic strain of P. yoelii, generated based on previous work⁵⁵, that expresses ookinete-stage-specific firefly luciferase was used. The infected blood was diluted into 10 ml ookinete culture medium and incubated for 20 h at 19 °C as described previously⁵⁶. Filtered bacterial supernatant (50 µl) was added to 500 µl of the ookinete suspension. The rate of ookinete inhibition was calculated either by counting ookinetes in a Giemsa-stained culture (P. berghei) or by monitoring the bioluminescent-signal intensity (P. yoelii) after adding 100 µg ml⁻¹ p-luciferin. Each sample was assayed in triplicate.

In vitro anti-*Plasmodium* activity assays of gametocyte-stage *P. falciparum*. A *P. falciparum* NF54 gametocyte culture was initiated at 0.5% asexual parasitaemia and 4% haematocrit, as previously described 57 . Bacteria were physically separated from parasites by a 0.22- μ m porous membrane using a Transwell system (Corning). Filtered bacterial suspension was added to the top chamber and the gametocyte culture was added to the bottom chamber. Gametocytaemia was determined three days post incubation. Over 1,000 erythrocytes were examined for gametocytes in Giemsa-stained blood films. The *Plasmodium* PI4K inhibitor KDU691 (20 μ M; ref. 58) was used as a positive control.

In vivo anti-ookinete formation assay of *P. falciparum*. *A. stephensi* mosquitoes carrying Su_YN1 wild type or the *AmLip*-KO mutant were fed with mature *P. falciparum* gametocytes and the mosquito midguts were dissected 20 h post blood feed. The blood bolus was spread on a glass slide and stained with Giemsa. Ookinetes in the midgut of individual mosquitoes were counted under microscopy.

Mass spectrometry-based proteomics of secreted proteins. The secreted proteomes of Su_YN1 and Su_JS3 were compared to identify protein components specifically produced by Su_YN1. The supernatants were filtered through a 0.22-µm membrane and collected for lysis in Laemmli sample buffer. The Su_YN1 and Su_JS3 supernatant proteins were then subjected to SDS-PAGE. After the samples were run 1 cm into the gel, all proteins were excised, digested in-gel and the resulting peptides were fractionated by HPLC for identification by mass spectrometry. The top eight abundant proteins enriched in Su_YN1 or Su_JS3 were selected for further screening.

Gene disruption and complementation. The genes encoding the differentially expressed proteins identified by mass spectrometry were deleted in the *S. ureilytica* Su_YN1 strain using the Red/ET method as described previously⁵⁹. Briefly, Su_YN1 was transformed by electro-transfection with the PSQ plasmid and the PSQ-carrying Su_YN1 cells were made competent for further transformation of recombinant DNA fragments targeting the genomic locus of interest. Gene disruption was confirmed by PCR and two knockout mutant *AmLip*-KO strains were selected to test for antimalarial activity. The sequences of the primers are listed in Supplementary Table 4.

Complemented strains were generated by introducing a plasmid carrying the disrupted gene into the AmLip-KO strain using electro-transformation. The AmLip coding region (with its 500-bp 5' untranslated region) was amplified and fused to a 3HA tag. Successful expression of AmLip was confirmed by western blotting using an anti-HA antibody. A S207A mutated version of AmLip was also introduced into the AmLip-KO strain.

Lipase-activity plate assay. The lipase activity of the bacterial culture supernatant and purified AmLip protein was measured using the egg yolk plate assay. and a specific and sensitive plate assay was used for bacterial lipases, as described previously. For the egg yolk plate assay, $10\,\mu$ l bacteria culture supernatant or 0.5–2 µg purified AmLip protein was spotted onto a 3% agar plate with 1% egg yolk and incubated for 20 h at 30 °C. Lipase activity was measured using the diameter of the lytic halo of each spot. For the specific and sensitive plate assay for triglyceride-lipase activity, bacterial culture supernatant or purified AmLip protein was spotted onto a 1% agar plate with 2% trioleoylglycerol (wt/vol) and 0.001% (wt/vol) rhodamine B and incubated for 20 h at 30 °C. Lipase activity was monitored by visualizing plates with 350 nm ultraviolet light.

Commercial antibodies. The commercial primary antibodies used were rabbit anti-HA (CST, cat. no. 3724S) and mouse anti-histone H3 (Abcam, ab1220). The commercial secondary antibodies used were goat anti-rabbit IgG horseradish peroxidase (HRP)-conjugated and goat anti-mouse IgG HRP-conjugated from Abcam, and Alexa 555 goat anti-rabbit IgG and Alexa 555 goat anti-mouse IgG from Thermo Fisher Scientific. For the western blot experiments, the rabbit anti-HA and mouse anti-histone H3 antibodies were used at a 1:1,000 dilution. The goat anti-rabbit IgG HRP-conjugated and goat anti-mouse IgG HRP-conjugated secondary antibodies were used at a 1:5,000 dilution. For immunofluorescence assays, the rabbit anti-HA antibody was used at a 1:500 dilution, and the Alexa 555 goat anti-rabbit IgG and Alexa 555 goat anti-mouse IgG secondary antibodies were used at a 1:500 dilution.

Recombinant AmLip purification and antiserum preparation. Recombinant AmLip was expressed and purified using the pET expression system. The AmLip coding sequence was PCR amplified, cloned into the NcoI and XhoI sites of the pET28a vector and protein was induced in *E. coli* BL21 by the auto-induction method⁴³. The protein was purified using HisPur Ni-NTA resin (Thermo Scientific) according to the manufacturer's instructions. AmLip mouse antiserum was prepared by immunizing ICR mice. The antiserum with good specificity was collected and stored at $-80\,^{\circ}\text{C}$ until use. The AmLip mouse antiserum were used at a 1:1,000 dilution for western blotting and 1:250 for immunofluorescence assays.

Haemolytic activity assay. Haemolytic activity was assayed by incubating the bacterial culture supernatant with erythrocytes as described previously 63 . Briefly, $50\,\mu l$ of the bacterial culture supernatant was added to a 48-well plate containing 1×10^8 red blood cells and incubated for 12h at 37 °C. After incubation, the culture was transferred to a 1.5 ml tube and centrifuged at 3,000 r.p.m. for 5 min. The supernatant (150 μl) was transferred to 96-well plates with a U-shaped bottom and absorbance was measured at 540 nm. Saponin (0.1% wt/vol) was used as a positive control.

Protein extraction and western blot analysis. Protein extraction from Serratia bacteria was performed using RIPA buffer plus complete protease inhibitor cocktail and 1 mM PMSE. After ultrasonication, the protein solution was centrifuged at 10,000g for 15 min at 4 °C. The supernatant was collected and Laemmli sample buffer was added. For protein extraction from Serratia culture supernatant, Laemmli sample buffer was added to the 0.22-µm-filtered culture, fractionated by 10% SDS-PAGE and transferred to a PVDF membrane. The membrane was blocked in blocking buffer (5% BSA in 1×TBST (Tris-buffered saline and Tween 20)) and incubated with primary antibodies. After incubation, the membrane was washed three times with TBST and incubated with HRP-conjugated secondary antibodies. The membrane was washed four times in TBST before enhanced chemiluminescence detection.

Immunofluorescence assays. After co-culture with *Serratia* culture supernatants, *Plasmodium* parasites were washed three times in PBS, fixed using 4% paraformaldehyde and transferred to a coverslip pretreated with poly-L-lysine. The fixed cells were then permeabilized by adding 0.1% Triton X-100 in PBS for 5 min. The detergent was removed with three washes with cold PBS and unspecific protein binding was blocked in 5% BSA solution for 60 min. The samples were incubated with the primary antibodies diluted in 3% BSA in PBS at 4 °C for 12 h.

Next, the cells were gently washed with cold PBS and incubated with fluorescently conjugated secondary antibodies for 1 h. The cells were washed with PBS, stained with the DNA dye Hoechst 33342, mounted in 90% glycerol solution and sealed with nail polish. Images were captured and processed using a Zeiss LSM 880 confocal microscope.

Evolutionary relationship of bacterial lipases. Bacteria lipase analysis was performed by alignment of 29 amino-acid sequences surrounding the Gly-X-Ser-X-Gly motif following previously work by Javed et al. with minor adaptions. The evolutionary history was inferred using the neighbour-joining method. The optimal tree with the sum of branch length = 10.15 is shown. The percentage of replicate trees in which the associated taxa clustered together in the bootstrap test (1,000 replicates) are shown next to the branches. The tree is drawn to scale, with branch lengths in the same units as those of the evolutionary distances used to infer the phylogenetic tree. The evolutionary distances were computed using the p-distance method. and are in the units of the number of amino-acid differences per site. The analysis involved 45 amino-acid sequences. Evolutionary analyses were conducted in MEGA7.

Extraction of antimalarial compounds from bacterial culture. Organic solvents of varying polarity were used to extract antimalarial compounds from bacterial culture. The solvents used were petroleum ether, ethyl acetate, chloroform and chloroform—methanol (2:1 vol/vol). The bacterial culture supernatant was extracted with an equal volume of organic solvent under ultrasonic treatment for 30 min. The organic-solvent phase was collected and vacuum dried. The extracted pellet was re-dissolved in dimethylsulfoxide and tested for antimalarial activity. The aqueous phase was also collected and vacuum treated for 20 min to remove contaminated organic solvents before being tested for antimalarial activity.

Vertical, venereal and trans-stadial transmission of Serratia. To test for vertical transmission, GFP-tagged Serratia bacteria were introduced into two-day-old adult female mosquitoes by feeding them on a cotton pad moistened with 5% sterile sucrose containing bacteria ($1\times10^7~cells~ml^{-1})$ for 24 h. The mosquitoes were fed on a healthy mouse three days after the introduction of bacteria and then allowed to lay eggs on damp filter paper in oviposition tubes two days post a blood meal, with each mosquito placed in an individual tube. The eggs were collected into a tube containing 300 μ l sterile $1\times PBS$ and homogenized. The bacterial load was determined by plating tenfold serial dilutions of the egg homogenates on LB agar plates containing $100~\mu g~ml^{-1}$ kanamycin and incubating the plates at 30 °C for 24 h. Fluorescent colonies were counted by fluorescence microscopy.

For male-to-female venereal transmission tests, GFP-tagged Serratia were introduced into newly emerged virgin male mosquitoes by feeding them on a cotton pad moistened with 5% sugar solution containing bacteria $(1\times10^7\,{\rm cells\,ml^{-1}})$ for 36 h. Twenty Serratia-carrying males were then allowed to mate with 20 three-day-old virgin females. Three days after mating, the mosquitoes were allowed to feed on blood and eggs were collected from individual females three days later. The spermatheca and laid eggs were examined for the presence of GFP-tagged Serratia bacteria by plating tenfold serial dilutions of the homogenates as described above.

To examine larva-to-adult trans-stadial transmission, GFP-tagged Serratia bacteria were introduced into mosquito larva by adding $500\,\mu l$ of a bacterial solution $(1\times 10^7\, cells\, ml^{-1})$ to $150\, ml$ of the larval breeding water. Three days after eclosion, 20-30 females were sampled and examined for GFP-marked bacteria in the female midgut by plating tenfold serial dilutions of the homogenates as described above.

Dissemination of Su_YN1 into mosquito populations in cage experiments. To test how efficiently S. ureilytica Su_YN1 bacteria spread through mosquito populations, we conducted laboratory cage experiments to measure the rates of Su_YN1-GFP dissemination in different stages of the mosquito life cycle as well as over multiple generations. Su YN1-GFP bacteria were introduced into newly emerged virgin male A. stephensi adult mosquitoes for 24 h. Ten Su_YN1-GFP-fed virgin males were mixed with 190 unfed virgin males and 200 uninfected virgin females in a laboratory cage. The introduced Su_YN1-GFP-fed mosquitoes constituted 5% of the total population. Two days later, the female mosquitoes were blood fed. Three days later, an oviposition cup was placed in the cage to collect eggs. Rearing of the larvae to adults followed standard protocol. A total of 30 fourth-instar larvae, and 30 male and 30 female adults were sampled and examined for the presence of fluorescent bacteria by plating larvae and adult midgut homogenates on LB agar plates containing kanamycin. To test the efficiency of Su YN1 transmission over multiple generations, the mosquitoes were reared and maintained for three consecutive generations. In each generation, 30 female adults were sampled and examined for the presence of GFP-tagged Su_YN1.

Statistical analysis. The statistical significance of the difference in oocyst number between bacteria- and PBS-fed mosquitoes (control) was analysed using a two-tailed Mann–Whitney test. The statistical significance between the survival data for *Serratia*- and PBS-fed mosquitoes (control) was analysed using a log-rank (Mantel–Cox) test. Other statistical significance was calculated using a Student's t-test or one-way analysis of variance. A value of P < 0.05 was regarded as

statistically significant. All statistics were performed using GraphPad Prism version 5.00 for Windows (GraphPad Software).

Reporting Summary. Further information on research design is available in the Nature Research Reporting Summary linked to this article.

Data availability

The entire 16S rRNA gene sequence dataset reported in this paper has been deposited in the National Center for Biotechnology Information Sequence Read Archive (accession no. PRJNA642229). This whole-genome shotgun project has been deposited at DDBJ/ENA/GenBank under the accession numbers JACAAS000000000, JACAAT000000000, JACAAU000000000 and JACAAV000000000. Source data are provided with this paper.

Received: 21 August 2020; Accepted: 29 March 2021; Published online: 6 May 2021

References

- 1. World Malaria Report (World Health Organization, 2019).
- Global Vector Control Response 2017–2030 (World Health Organization, 2017).
- Dondorp, A. M. et al. Artemisinin resistance: current status and scenarios for containment. Nat. Rev. Microbiol. 8, 272–280 (2010).
- Ranson, H. & Lissenden, N. Insecticide resistance in African Anopheles mosquitoes: a worsening situation that needs urgent action to maintain malaria control. Trends Parasitol. 32, 187–196 (2016).
- Hamilton, W. L. et al. Evolution and expansion of multidrug-resistant malaria in southeast Asia: a genomic epidemiology study. *Lancet Infect. Dis.* 19, 943–951 (2019).
- van der Pluijm, R. W. et al. Determinants of dihydroartemisinin-piperaquine treatment failure in *Plasmodium falciparum* malaria in Cambodia, Thailand, and Vietnam: a prospective clinical, pharmacological, and genetic study. *Lancet Infect. Dis.* 19, 952–961 (2019).
- Imwong, M., Hien, T. T., Thuy-Nhien, N. T., Dondorp, A. M. & White, N. J. Spread of a single multidrug resistant malaria parasite lineage (PfPailin) to Vietnam. *Lancet Infect. Dis.* 17, 1022–1023 (2017).
- Haldar, K., Bhattacharjee, S. & Safeukui, I. Drug resistance in *Plasmodium*. Nat. Rev. Microbiol. 16, 156–170 (2018).
- Bhatt, S. et al. The effect of malaria control on *Plasmodium falciparum* in Africa between 2000 and 2015. *Nature* 526, 207–211 (2015).
- Alonso, P. L. & Tanner, M. Public health challenges and prospects for malaria control and elimination. Nat. Med. 19, 150–155 (2013).
- 11. Talapko, J., Skrlec, I., Alebic, T., Jukic, M. & Vcev, A. Malaria: the past and the present. *Microorganisms* 7, 179 (2019).
- 12. Vythilingam, I. & Hii, J. in Anopheles Mosquitoes—New Insights into Malaria Vectors (ed. Manguin, S.) 1st edn (InTech, 2013).
- Ghosh, A., Edwards, M. J. & Jacobs-Lorena, M. The journey of the malaria parasite in the mosquito: hopes for the new century. *Parasitol. Today* 16, 196–201 (2000).
- Simon, N. et al. Sexual stage adhesion proteins form multi-protein complexes in the malaria parasite *Plasmodium falciparum*. J. Biol. Chem. 284, 14537–14546 (2009).
- Pradel, G. Proteins of the malaria parasite sexual stages: expression, function and potential for transmission blocking strategies. *Parasitology* 134, 1911–1929 (2007).
- Sinden, R. E., Alavi, Y. & Raine, J. D. Mosquito–malaria interactions: a reappraisal of the concepts of susceptibility and refractoriness. *Insect Biochem. Mol. Biol.* 34, 625–629 (2004).
- 17. Boissiere, A. et al. Midgut microbiota of the malaria mosquito vector *Anopheles gambiae* and interactions with *Plasmodium falciparum* infection. *PLoS Pathog.* **8**, e1002742 (2012).
- Heu, K. & Gendrin, M. Mosquito microbiota and its influence on disease vectorial transmission (in French). Biol. Aujourdhui 212, 119–136 (2018).
- Wilke, A. B. B. & Marrelli, M. T. Paratransgenesis: a promising new strategy for mosquito vector control. *Parasit. Vectors* 8, 342 (2015).
- Coutinho-Abreu, I. V., Zhu, K. Y. & Ramalho-Ortigao, M. Transgenesis and paratransgenesis to control insect-borne diseases: current status and future challenges. *Parasitol. Int.* 59, 1–8 (2010).
- Wang, S. et al. Fighting malaria with engineered symbiotic bacteria from vector mosquitoes. *Proc. Natl Acad. Sci. USA* 109, 12734–12739 (2012).
- Wang, S. & Jacobs-Lorena, M. Genetic approaches to interfere with malaria transmission by vector mosquitoes. *Trends Biotechnol.* 31, 185–193 (2013).
- Bahia, A. C. et al. Exploring Anopheles gut bacteria for Plasmodium blocking activity. Environ. Microbiol. 16, 2980–2994 (2014).
- 24. Wang, S. et al. Driving mosquito refractoriness to *Plasmodium falciparum* with engineered symbiotic bacteria. *Science* **357**, 1399–1402 (2017).
- Cirimotich, C. M. et al. Natural microbe mediated refractoriness to Plasmodium infection in Anopheles gambiae. Science 332, 855–858 (2011).

 Gao, H., Cui, C., Wang, L., Jacobs-Lorena, M. & Wang, S. Mosquito microbiota and implications for disease control. *Trends Parasitol.* 36, 98–111 (2020).

- Dong, Y. M., Manfredini, F. & Dimopoulos, G. Implication of the mosquito midgut microbiota in the defense against malaria parasites. *PLoS Pathog.* 5, e1000423 (2009).
- Angkawidjaja, C. & Kanaya, S. Family I.3 lipase: bacterial lipases secreted by the type I secretion system. Cell Mol. Life Sci. 63, 2804–2817 (2006).
- Arpigny, J. L. & Jaeger, K.-E. Bacterial lipolytic enzymes: classification and properties. *Biochem. J.* 343, 177–183 (1999).
- Osei-Poku, J., Mbogo, C. M., Palmer, W. J. & Jiggins, F. M. Deep sequencing reveals extensive variation in the gut microbiota of wild mosquitoes from Kenya. Mol. Ecol. 21, 5138–5150 (2012).
- Wang, Y., Gilbreath, T. M. III, Kukutla, P., Yan, G. & Xu, J. Dynamic gut microbiome across life history of the malaria mosquito *Anopheles gambiae* in Kenya. *PLoS ONE* 6, e24767 (2011).
- Bando, H. et al. Intra-specific diversity of Serratia marcescens in Anopheles mosquito midgut defines Plasmodium transmission capacity. Sci. Rep. 3, 1641 (2013).
- Pumpuni, C. B., Demaio, J., Kent, M., Davis, J. R. & Beier, J. C. Bacterial population dynamics in three anopheline species: the impact on *Plasmodium* sporogonic development. *Am. J. Trop. Med Hyg.* 54, 214–218 (1996).
- 34. Rani, A., Sharma, A., Rajagopal, R., Adak, T. & Bhatnagar, R. K. Bacterial diversity analysis of larvae and adult midgut microflora using culture-dependent and culture-independent methods in lab-reared and field-collected *Anopheles stephensi*—an Asian malarial vector. *BMC Microbiol.* 9, 1471–2180 (2009).
- Gonzalez-Ceron, L., Santillan, F., Rodriguez, M. H., Mendez, D. & Hernandez-Avila, J. E. Bacteria in midguts of field-collected *Anopheles albimanus* block *Plasmodium vivax* sporogonic development. *J. Med. Entomol.* 40, 371–374 (2003).
- 36. Villegas, L. M. & Pimenta, P. F. P. Metagenomics, paratransgenesis and the Anopheles microbiome: a portrait of the geographical distribution of the anopheline microbiota based on a meta-analysis of reported taxa. Mem. Inst. Oswaldo Cruz 109, 672–684 (2014).
- Bai, L., Wang, L., Vega-Rodriguez, J., Wang, G. & Wang, S. A gut gymbiotic bacterium Serratia marcescens renders mosquito resistance to Plasmodium infection through activation of mosquito immune responses. Front. Microbiol. 10, 1580 (2019).
- Garcia, C. J. et al. Serralysin family metalloproteases protects Serratia marcescens from predation by the predatory bacteria Micavibrio aeruginosavorus. Sci. Rep. 8, 14025 (2018).
- Mitamura, T. & Palacpac, N. M. Q. Lipid metabolism in *Plasmodium falciparum*-infected erythrocytes: possible new targets for malaria chemotherapy. *Microbes Infect.* 5, 545–552 (2003).
- Zhu, G. et al. Susceptibility of Anopheles sinensis to Plasmodium vivax in malarial outbreak areas of central China. Parasit. Vectors 6, 176 (2013).
- 41. Bolger, A. M., Lohse, M. & Usadel, B. Trimmomatic: a flexible trimmer for Illumina sequence data. *Bioinformatics* **30**, 2114–2120 (2014).
- 42. Reyon, D. et al. FLASH assembly of TALENs for high-throughput genome editing. *Nat. Biotechnol.* **30**, 460–465 (2012).
- Caporaso, J. G. et al. QIIME allows analysis of high-throughput community sequencing data. Nat. Methods 7, 335–336 (2010).
- 44. Rognes, T., Flouri, T., Nichols, B., Quince, C. & Mahe, F. VSEARCH: a versatile open source tool for metagenomics. *PeerJ* 4, e2584 (2016).
- Wang, Q., Garrity, G. M., Tiedje, J. M. & Cole, J. R. Naive Bayesian classifier for rapid assignment of rRNA sequences into the new bacterial taxonomy. *Appl. Environ. Microbiol.* 73, 5261–5267 (2007).
- Kumar, S., Stecher, G. & Tamura, K. MEGA7: Molecular Evolutionary Genetics Analysis version 7.0 for bigger datasets. *Mol. Biol. Evol.* 33, 1870–1874 (2016).
- Berlin, K. et al. Assembling large genomes with single-molecule sequencing and locality-sensitive hashing. Nat. Biotechnol. 33, 623–630 (2014).
- Chen, F., Mackey, A. J., Vermunt, J. K. & Roos, D. S. Assessing performance of orthology detection strategies applied to eukaryotic genomes. PLoS ONE 2, e383 (2007)
- Edgar, R. C. MUSCLE: multiple sequence alignment with high accuracy and high throughput. *Nucleic Acids Res.* 32, 1792–1797 (2004).
- Capella-Gutierrez, S., Silla-Martinez, J. M. & Gabaldon, T. trimAl: a tool for automated alignment trimming in large-scale phylogenetic analyses. *Bioinformatics* 25, 1972–1973 (2009).
- Guindon, S. et al. New algorithms and methods to estimate maximum-likelihood phylogenies: assessing the performance of PhyML 3.0. Syst. Biol. 59, 307–321 (2010).
- Abascal, F., Zardoya, R. & Posada, D. ProtTest: selection of best-fit models of protein evolution. *Bioinformatics* 21, 2104–2105 (2005).
- Wei, G. et al. Insect pathogenic fungus interacts with the gut microbiota to accelerate mosquito mortality. *Proc. Natl Acad. Sci. USA* 114, 5994–5999 (2017).

- 54. Sinden, R. E. et al. Ookinete antigens of *Plasmodium berghei*: a light and electron-microscope immunogold study of expression of the 21 kDa determinant recognized by a transmission-blocking antibody. *Proc. R. Soc. Lond. B Biol. Sci.* 230, 443–458 (1987).
- De Niz, M., Stanway, R. R., Wacker, R., Keller, D. & Heussler, V. T. An ultrasensitive NanoLuc-based luminescence system for monitoring *Plasmodium berghei* throughout its life cycle. *Malar. J.* 15, 232–232 (2016).
- Gao, H. et al. ISP1-anchored polarization of GCβ/CDC50A complex initiates malaria ookinete gliding motility. Curr. Biol. 28, 2763–2776 (2018).
- Kumar, S., Molina-Cruz, A., Gupta, L., Rodrigues, J. & Barillas-Mury, C. A peroxidase/dual oxidase system modulates midgut epithelial immunity in *Anopheles. Science* 327, 1644–1648 (2010).
- McNamara, C. W. et al. Targeting *Plasmodium* PI(4)K to eliminate malaria. *Nature* 504, 248–253 (2013).
- Huang, H., Song, X. & Yang, S. Development of a RecE/T-Assisted CRISPR-Cas9 toolbox for *Lactobacillus*. *Biotechnol. J.* 14, e1800690 (2019).
- Liu, P. C., Lee, K. K. & Chen, S. N. Pathogenicity of different isolates of Vibrio harveyi in tiger prawn, Penaeus monodon. Lett. Appl. Microbiol. 22, 413–416 (1996).
- Kourker, G. & Jaeger, K. E. Specific and sensitive plate assay for bacterial lipases. Appl. Environ. Microbiol. 53, 211–213 (1987).
- Studier, F. W. Protein production by auto-induction in high density shaking cultures. Protein Expr. Purif. 41, 207–234 (2005).
- Fantappie, L. et al. Antibody-mediated immunity induced by engineered *Escherichia coli* OMVs carrying heterologous antigens in their lumen.
 J. Extracell. Vesicles https://doi.org/10.3402/jev.v3.24015 (2014).
- Peach, M., Marsh, N., Miskiewicz, E. I. & MacPhee, D. J. in Western Blotting: Methods and Protocols (eds Kurien, B. T. & Scofield, R. H.) 49–60 (Springer New York, 2015).
- Javed, S. et al. Bacterial lipases: a review on purification and characterization. Prog. Biophys. Mol. Biol. 132, 23–34 (2018).
- Saitou, N. & Nei, M. The neighbor-joining method: a new method for reconstructing phylogenetic trees. Mol. Biol. Evol. 4, 406–425 (1987).
- Felsenstein, J. Confidence limits on phylogenies: an approach using the bootstrap. Evolution 39, 783–791 (1985).
- 68. Nei, M., & Kumar, S. Molecular Evolution and Phylogenetics (Oxford University Press, 2000).

Acknowledgements

This work was supported by grants from the National Natural Science Foundation of China (grants nos. 31830086, 32021001 and 31472044) to S.W.; the National Key R&D

Program of China (grant no. 2019YFC1200800) to S.W.; the Strategic Priority Research Program of the Chinese Academy of Sciences (grant no. XDB11010500) to S.W.; the Key Research Program of the Chinese Academy of Sciences (grant no. KFZD-SW-219) to S.W.; the National Institutes of Health (grant no. R01A1031478) to M.J.-L.; the Johns Hopkins Malaria Research Institute Insectary, Parasite Core Facilities; the Bloomberg Philanthropies and the Jiangsu Provincial Department of Science and Technology (grant no. BM2018020) to J.C. We thank F. Li for rearing mosquitoes.

Author contributions

S.W. conceived the project. S.W., H.G. and L.B. designed the study. L.B., X.L., S.L., G.Z. and J.C. collected wild mosquitoes. L.B. conducted the gut symbiotic bacteria isolation, gut colonization, RNA interference and effects of isolated bacteria on *P. berghei* infection and mosquito biology assays. L.B. and X.L. performed the *A. sinensis* susceptibility on *P. vivax* infection assays. H.G. conducted the in vitro anti-*Plasmodium* activity, mass spectrometry, gene disruption, western blot, Am.Lip-mediated anti-*Plasmodium* activity and immunofluorescence assays. Y.J. conducted the bacterial transmission and cage experiments. W.H. conducted assays to determine the effect of *Serratia* bacteria on *P. falciparum* infection. Z.H. and L.B. investigated the effect of *Serratia* culture supernatant on *P. falciparum* gametocyte development. D.W. provided *P. vivax* epidemic data. S.Z. performed phylogenomic analysis. L.J. and M.J.-L. provided materials. H.G., L.B. and S.W. analysed the data. H.G., L.W. and S.W. wrote the manuscript. M.J.-L. and S.W. edited the manuscript.

Competing interests

The authors declare no competing interests.

Additional information

Extended data is available for this paper at https://doi.org/10.1038/s41564-021-00899-8.

Supplementary information The online version contains supplementary material available at https://doi.org/10.1038/s41564-021-00899-8.

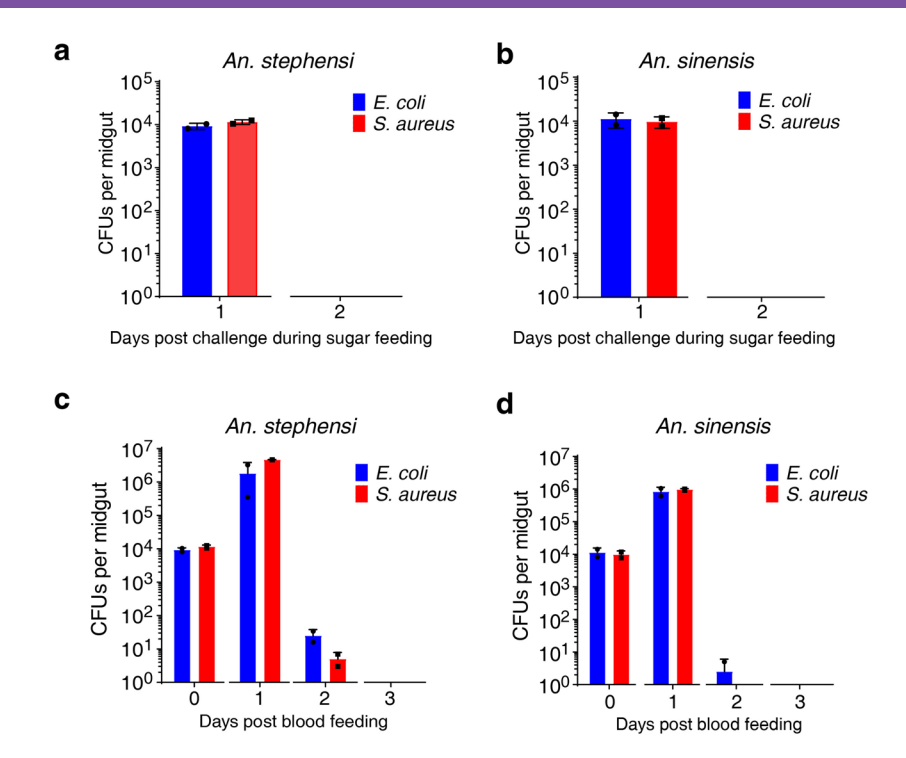
Correspondence and requests for materials should be addressed to S.W.

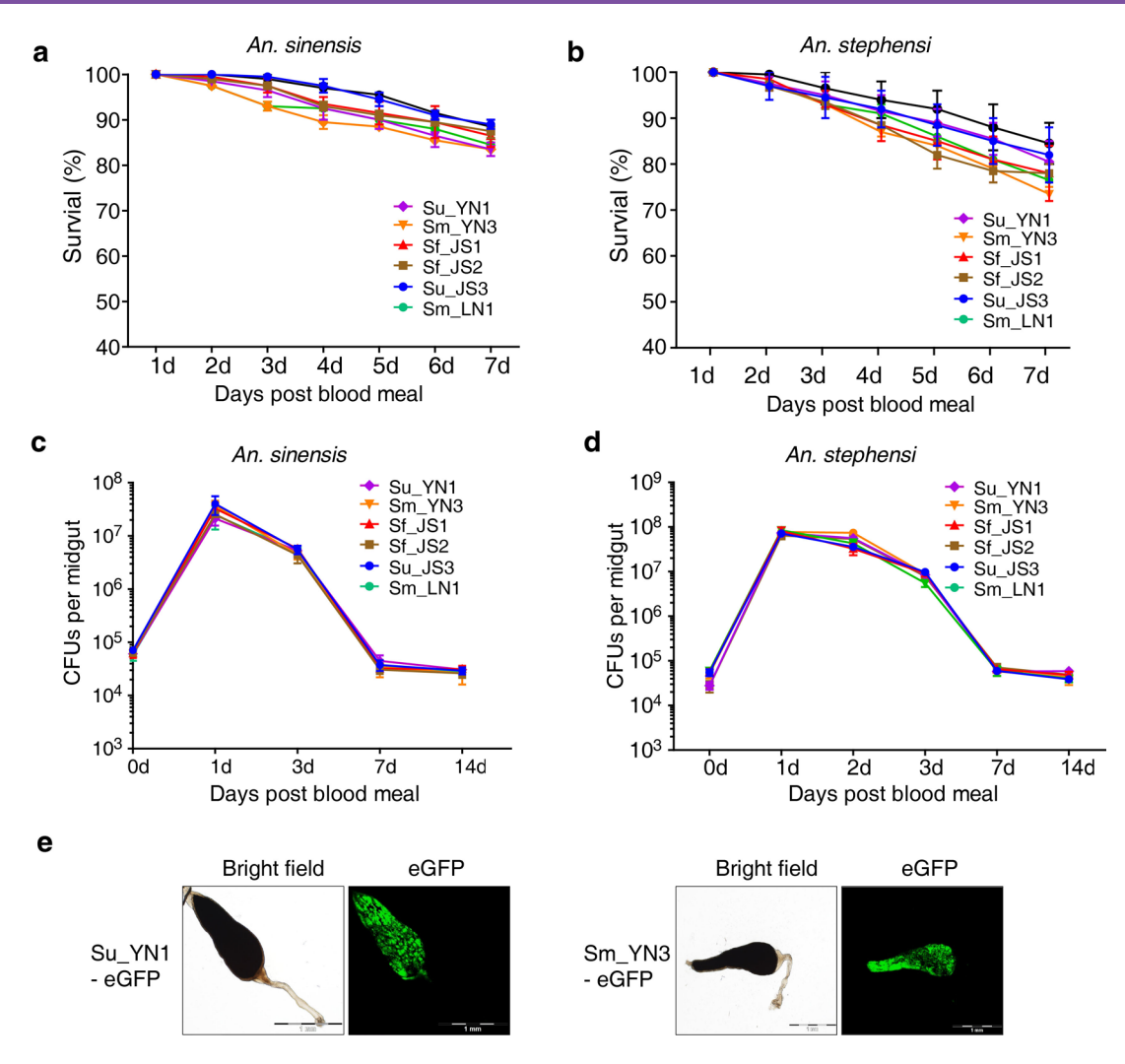
Peer review information Nature Microbiology thanks Hitotaka Kanuka and the other, anonymous, reviewer(s) for their contribution to the peer review of this work. Peer reviewer reports are available.

Reprints and permissions information is available at www.nature.com/reprints.

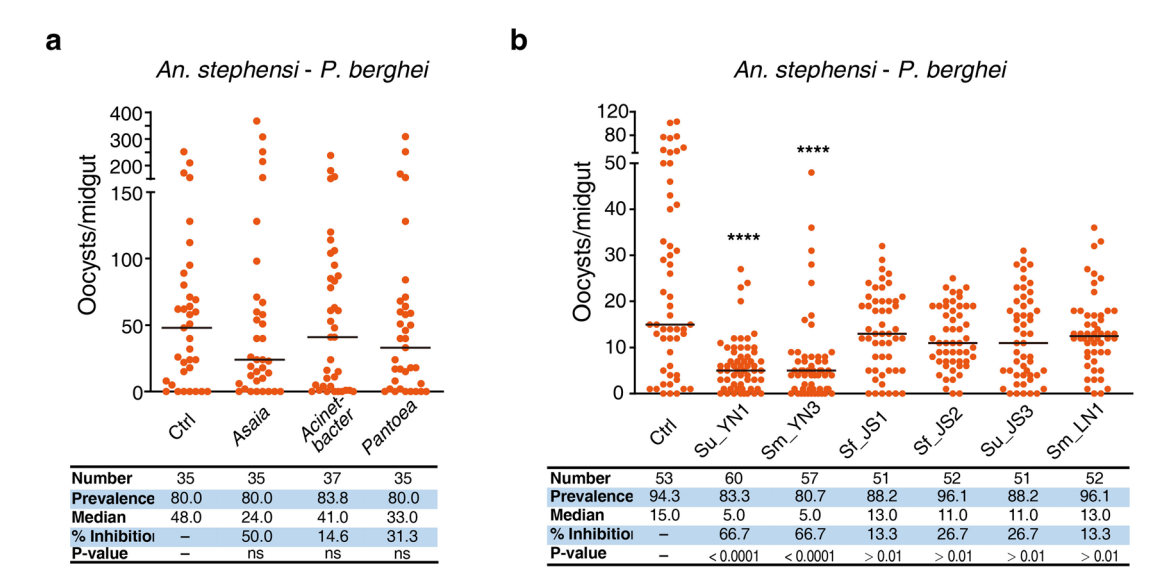
Publisher's note Springer Nature remains neutral with regard to jurisdictional claims in published maps and institutional affiliations.

© The Author(s), under exclusive licence to Springer Nature Limited 2021



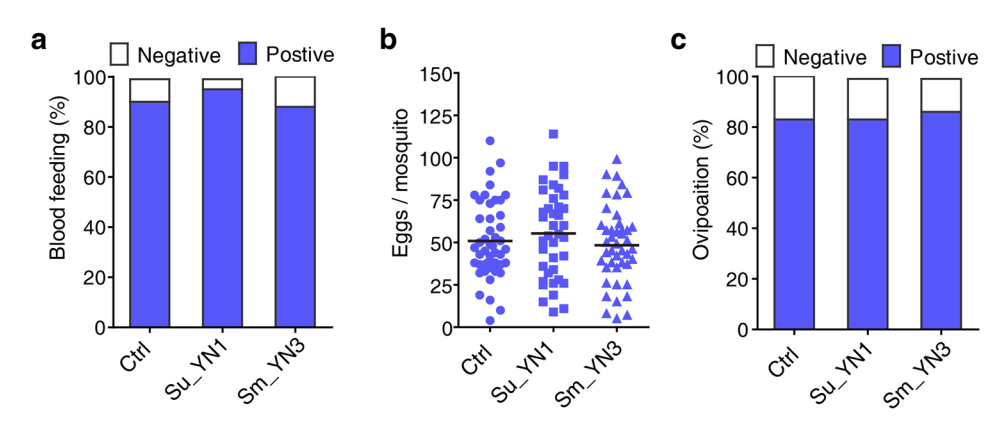


Extended Data Fig. 2 | Serratia strains stably colonize the mosquito midgut and do not impact mosquito longevity. **a**, **b**, Effect of Serratia strains on An. sinensis (**a**) and An. stephensi (**b**) survival post blood meal. Bacteria were administered to two-day-old female mosquitoes via sugar meal and then fed blood. Survival was monitored daily. Data points are mean \pm s.d. The dots represent biologically independent replicates (n = 2). Each replicate contains 10 mosquito midguts. **c**,**d**, Serratia bacteria numbers in the midgut of female An. sinensis (**c**) and An. stephensi (**d**) post blood meal. Data points are mean \pm s.d. The dots represent biologically independent replicates (n = 2). Each replicate contains 10 mosquito midguts. **e**, Visualization of GFP-tagged Su_YN1 and Sm_YN3 bacteria in the midgut of An. stephensi at 24 h after a blood meal. Bright-field images (left) are paired with the corresponding fluorescent images (right). The experiments were repeated twice with similar results.

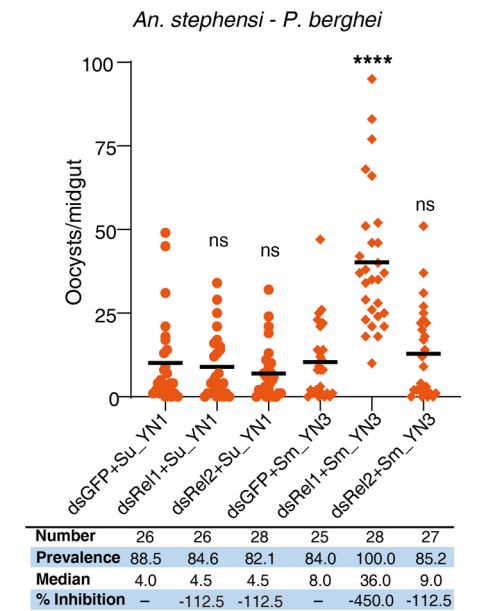


Extended Data Fig. 3 | Effect of bacteria on *P. berghei* oocyst formation in *An. stephensi.* **a**, *P. berghei* oocyst load in *An. stephensi* mosquitoes carrying *Asaia, Acinetobacter* or *Pantoea* bacteria from YN wild caught mosquitoes. **b**, *P. berghei* oocyst load in *An. stephensi* mosquitoes fed with different *Serratia* strains from different wild-caught mosquito populations. Circles represent the number of oocysts in individual midguts, and horizontal lines indicate the median number of oocysts per midgut. The sample size (n Number) of each group is listed in the table of the lower panel. The statistical significance of the oocyst intensity between the bacteria-fed mosquitoes and PBS-fed mosquitoes (Ctrl) was analysed using the two-tailed Mann-Whitney test.

*****P < 0.0001, *P* > 0.05, not significant (ns). The exact *P* values in (**a**) were as follows: *Asaia*, 0.4508; *Acinetobacter*, 0.8728; *Pantoea*, 0.4265. The exact *P* values in (b) were as follows: Su_YN1, < 0.0001; Sm_YN3, < 0.0001; Sf_JS1, 0.0271; Sf_JS2, 0.0135; Su_JS3, 0.0117; Sm_LN1, 0.0220.



Extended Data Fig. 4 | The effect of Serratia Su_YN1 and Sm_YN3 on An. stephensi blood feeding, fecundity and oviposition rate. Serratia Su_YN1 and Sm_YN3 do not impact An. stephensi mosquito blood feeding behaviour (n=100 mosquitoes each group) (a), egg production (Ctrl, n=46, Su_YN1, n=39, Sm_YN3, n=44) (b) or oviposition rate (n=100 mosquitoes each group) c, Two-day-old An. stephensi mosquitoes were fed on a sugar meal containing bacteria or 5% sugar alone (Ctrl). Three days later, female mosquitoes were fed on a mouse and three days later eggs were collected from individual females. The experiments were repeated three times with similar results. No significant differences were detected among the groups (one-way ANOVA or two-tailed Mann-Whitney test).



Extended Data Fig. 5 | Effect of *Rel1* and *Rel2* silencing on Su_YN1- or Sm_YN3-mediated anti-*Plasmodium* activity. *Rel1* and *Rel2* were silenced in *An. stephensi* by systemic injection of double-stranded RNA dsRel1, dsRel2 or dsGFP. The injected mosquitoes were fed on a sugar meal containing Su_YN1 or Sm_YN3. Three days later, the mosquitoes were allowed to feed on the same *P. berghei* infected mouse. The injected double-stranded RNA (ds) and presence of bacteria are indicated below each column. Each dot represents the oocyst number of an individual midgut, and the horizontal lines indicate the median number of oocysts per midgut. Data are from n = 25 to 28 mosquitoes per group. The sample size (n Number) of each group is listed in the table of the lower panel. The statistical significance of oocyst intensity differences between the dsRel1- or dsRel2-injected and dsGFP-injected mosquitoes carrying the same bacteria (Su_YN1 or Sm_YN3) was analysed using the two-tailed Mann-Whitney test. *****P < 0.0001, P > 0.05, not significant (ns). The exact values were as follows: dsRel1+Su_YN1, 0.8519; dsRel2+Su_YN1, 0.5605; dsRel1+Sm_YN3, <0.0001; sRel2+Sm_YN3, 0.4851.

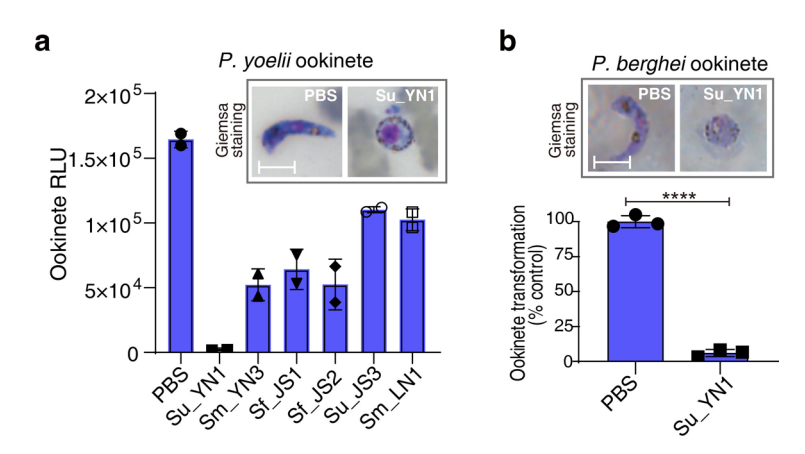
ns

ns

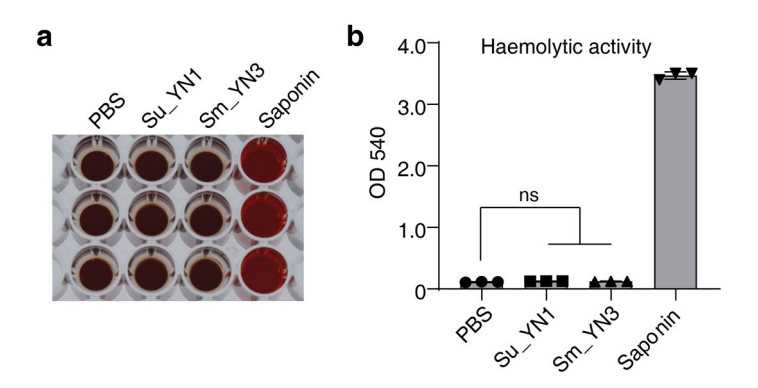
< 0.0001

ns

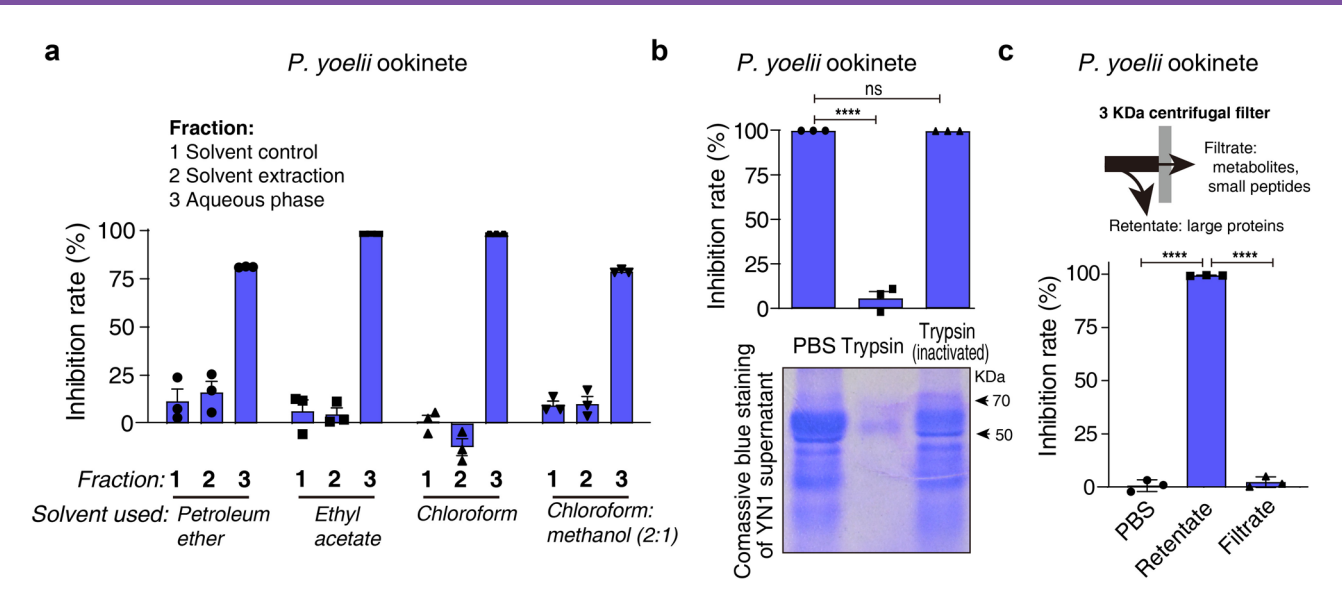
P-value



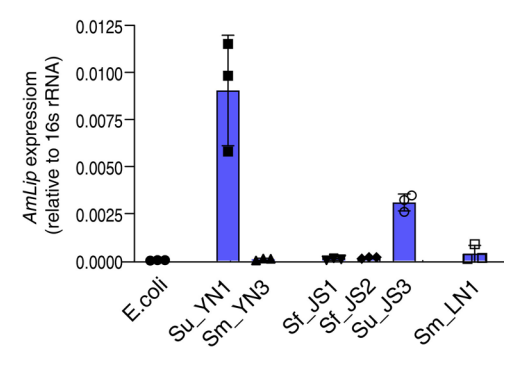
Extended Data Fig. 6 | Su_YN1 culture supernatant inhibited *P. berghei* **ookinete formation. a**, Inhibition by *Serratia* culture supernatants of *P. yoelii* ookinete formation *in vitro*. Ookinete formation was quantified by luminescence measurements using the *Py.*17XNL reporter strain. RLU, relative light units. The experiments were repeated three times with similar results. Data points are mean \pm s.d. The dots represent biologically independent replicates (n = 2). b, Effect of Su_YN1 culture supernatant on *P. berghei* ookinete formation *in vitro* assay using Giemsa staining. Transformation rate was quantified by comparison with the PBS control. The experiments were repeated three times with similar results. Data points are mean \pm s.d. The dots represent biologically independent replicates (n = 3). Statistical significance of the ookinete transformation rate was compared with the PBS control using two-tailed Student's *t*-test, *****P < 0.0001. The exact *P* value was, < 0.0001.



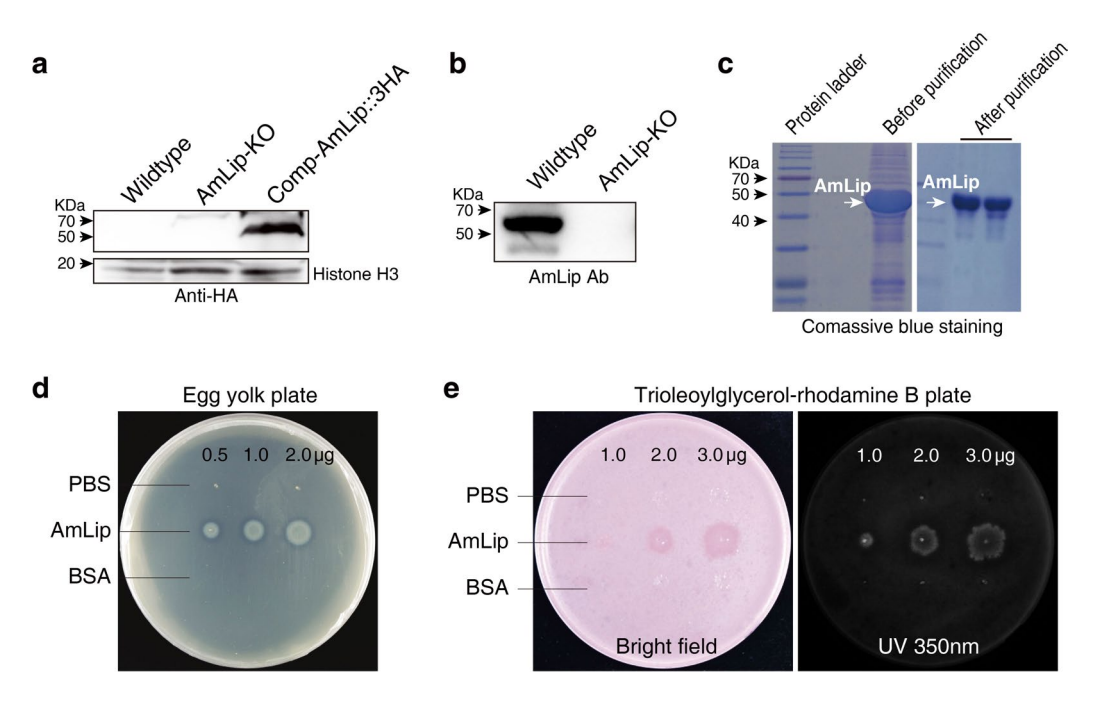
Extended Data Fig. 7 | Haemolytic activity assay of Su_YN1 and Sm_YN3. a, Bacteria culture supernatant was added (10% V/V) and the mixture incubated with erythrocytes for 12 h. **b**, The supernatants were collected and the absorbance at 540 nm was measured to evaluate haemoglobin release. Saponin was used as a haemolytic positive control. Data points are mean \pm s.d. The dots represent biologically independent replicates (n=3). Statistical significance of haemolytic activity was compared with the PBS control using two-tailed Student's *t*-test. *P* > 0.05, not significant (ns). The exact *P* values were as follows: Su_YN1, 0.1672; Sm_YN3, 0.3754.



Extended Data Fig. 8 | Antimalarial activity of different Su_YN1 culture supernatant fractions. a, Antimalarial activity of organic solvent extracts. Su_YN1 culture supernatant was extracted with solvents of various polarities. The extracted fractions were dried and dissolved in DMSO and the remaining aqueous phase was vacuum treated to remove residual organic reagents. All fractions were tested for antimalarial activity. **b**, Antimalarial activity assay of Su_YN1 culture supernatant separated using a 3 kDa cut-off centrifugal filter. The retentate and the filtrate were tested. **c**, Trypsin digestion of Su_YN1 culture supernatant abolishes antimalarial activity. Coomassie Brilliant Blue staining in the lower panel shows the protein patterns before and after treatment. Data points in (**b**) and (**c**) are mean \pm s.d. The dots represent biologically independent replicates (n = 3). Statistical significance of the ookinete inhibition rate was compared with the PBS control using two-tailed Student's t-test, ****P < 0.0001, P > 0.05, not significant (ns). The exact P values in (**b**) were: Trypsin, < 0.0001; Trypsin-inactivated, 0.0552. The exact P values in (**c**) were: Retentate (compared with PBS), < 0.0001; Filtrate (compared with Retentate), < 0.0001.



Extended Data Fig. 9 | AmLip gene expression in different Serratia strains. Detection of AmLip transcript abundance in different Serratia strains by qRT-PCR using Serratia 16 s rRNA as an internal reference. Data points are mean \pm s.d. The dots represent biologically independent replicates (n = 3). The experiments were repeated twice with similar results.



Extended Data Fig. 10 | Synthesis and purification of Serratia AmLip protein. a, Western blot detection using HA antibody, of 3HA-tagged AmLip protein in bacterial extracts of Su_YN1 wild type, knock-out mutant AmLip-KO and a mutant AmLip-KO complemented with the AmLip:HA gene. The experiments were repeated twice with similar results. **b**, Knockout of *AmLip* was verified by Western blot assay using an AmLip mouse antiserum. The experiments were repeated twice with similar results. **c**, Expression and purification of AmLip protein expressed *E. coli* BL21 (DE3). Coomassie blue staining showing the AmLip protein before and after purification on a nickel column. The experiments were repeated twice with similar results. **d**, Lipase activity test of the purified AmLip protein using the egg yolk lipoprotein plate degradation assay. **e**, Lipase activity assay of the purified AmLip protein using the trioleoylglycerol- rhodamine B plate degradation assay.

nature research

Corresponding author(s):	Sibao Wang
Last updated by author(s):	Mar 22, 2021

Reporting Summary

Nature Research wishes to improve the reproducibility of the work that we publish. This form provides structure for consistency and transparency in reporting. For further information on Nature Research policies, see our Editorial Policies and the Editorial Policy Checklist.

For all statistical analyses, confirm that the following items are present in the figure legend, table legend, main text, or Methods section

_				
St	ta:	tie	cti	2

	an otationoar an	any sees, seeman and the reme and present in the regard, table regard, main tends of methods seemen.		
n/a	Confirmed			
	The exact	The exact sample size (n) for each experimental group/condition, given as a discrete number and unit of measurement		
	A stateme	nt on whether measurements were taken from distinct samples or whether the same sample was measured repeatedly		
	The statistical test(s) used AND whether they are one- or two-sided Only common tests should be described solely by name; describe more complex techniques in the Methods section.			
\boxtimes	A description of all covariates tested			
\boxtimes	A descript	ion of any assumptions or corrections, such as tests of normality and adjustment for multiple comparisons		
	A full description of the statistical parameters including central tendency (e.g. means) or other basic estimates (e.g. regression coefficient) AND variation (e.g. standard deviation) or associated estimates of uncertainty (e.g. confidence intervals)			
	For null hypothesis testing, the test statistic (e.g. <i>F</i> , <i>t</i> , <i>r</i>) with confidence intervals, effect sizes, degrees of freedom and <i>P</i> value noted Give <i>P</i> values as exact values whenever suitable.			
\boxtimes	For Bayesian analysis, information on the choice of priors and Markov chain Monte Carlo settings			
\boxtimes	For hierarchical and complex designs, identification of the appropriate level for tests and full reporting of outcomes			
\square Estimates of effect sizes (e.g. Cohen's d , Pearson's r), indicating how they were calculated				
Our web collection on <u>statistics for biologists</u> contains articles on many of the points above.				
Software and code				
Poli	cy information a	about <u>availability of computer code</u>		
D	ata collection	No software was used for data collection.		
Da	ata analysis	All statistics were performed using GraphPad Prism version 5.00 for Windows. Circos plot showing that Serratia bacteria distribution was constructed using online tool Circos (mkweb.bcgsc.ca/tableviewer/visualize/). Phylogenomic analysis of bacterial whole-genome sequences was constructed using PhyMI softwarev 3.0.		

For manuscripts utilizing custom algorithms or software that are central to the research but not yet described in published literature, software must be made available to editors and reviewers. We strongly encourage code deposition in a community repository (e.g. GitHub). See the Nature Research guidelines for submitting code & software for further information.

Data

Policy information about availability of data

All manuscripts must include a data availability statement. This statement should provide the following information, where applicable:

- Accession codes, unique identifiers, or web links for publicly available datasets

Evolutionary analyses of bacterial lipases were conducted in MEGA7.0.26.

- A list of figures that have associated raw data
- A description of any restrictions on data availability

The entire 16S rRNA gene sequence dataset reported in this paper has been deposited in the National Center for Biotechnology Information Sequence Read Archive (accession no. PRJNA642229). (https://www.ncbi.nlm.nih.gov/bioproject/PRJNA642229). This Whole Genome Shotgun project has been deposited at DDBJ/ENA/GenBank under the accession JACAAS000000000, JACAAT0000000000, JACAAU0000000000, JACAAV000000000. Source data are provided with this paper.

Field-specific reporting				
Please select the or	ne below that is the best fit for your research. If you are not sure, read the appropriate sections before making your selection. Behavioural & social sciences Ecological, evolutionary & environmental sciences he document with all sections, see nature.com/documents/nr-reporting-summary-flat.pdf			
Life scier	nces study design			
All studies must dis	close on these points even when the disclosure is negative.			
Sample size	Sample sizes were empirically determined to optimize numbers based on our and others' previous experience with equivalent experiments [see for example Wang et al. Science. 371, 411–415 (2021)].			
Data exclusions	No data were excluded.			
Replication	All findings described in the paper were confirmed by repeating experiments as indicated in the figure legends and, when possible/ applicable, performing distinct experiments to support the same experimental finding.			
Randomization	The same batch of adult mosquitoes were allocated randomly to different groups in each test. The same batch of diluted parasites solutions were divided in equal amounts for each inhibition assay.			
Blinding	Blinding was not relevant to this study.			
Reporting for specific materials, systems and methods We require information from authors about some types of materials, experimental systems and methods used in many studies. Here, indicate whether each material, system or method listed is relevant to your study. If you are not sure if a list item applies to your research, read the appropriate section before selecting a response. Materials & experimental systems Methods Na Involved in the study ChIP-seq Antibodies Flow cytometry Flow cytometry Palaeontology and archaeology MRI-based neuroimaging Animals and other organisms Human research participants Clinical data Dual use research of concern				
Antibodies				
Antibodies used	Rabbit monoclonal anti-HA CST Cat# 3724S (use at 1:1000 for WB and 1:500 for IFA) Mouse monoclonal anti-Histone H3 Abcam Cat# ab1220 (use at 1:1000 for WB) Goat polyclonal anti-rabbit IgG, HRP conjugated Abcam Cat# ab6721 (use at 1:5000 for WB) Goat polyclonal anti-mouse IgG, HRP conjugated Abcam Cat# ab97023 (use at 1:5000 for WB) Goat polyclonal anti-Rabbit IgG, Alexa Fluor 555 conjugated Thermo Cat# A27039 (use at 1:5000 for IFA) Goat polyclonal anti-mouse IgG, Alexa Fluor 555 conjugated Thermo Cat# A21422 (use at 1:5000 for IFA)			
Validation	When possible, antibodies were validated by including positive and/or negative controls in the experiments themselves. Otherwise we relied on the validation data provided by the supplier.			
Eukaryotic c	ell lines			
Policy information about <u>cell lines</u>				
Cell line source(s) Plasmodium falciparum cell line NF54 and 3D7, Plasmodium berghei cell line ANKA and Plasmodium yoelii cell line 3 were obtained from Johns Hopkins University.				

Policy information about <u>cell lines</u>	
Cell line source(s)	Plasmodium falciparum cell line NF54 and 3D7, Plasmodium berghei cell line ANKA and Plasmodium yoelii cell line 17XNL were obtained from Johns Hopkins University.
Authentication	N/A
Mycoplasma contamination	Cell lines were not contaminated by mycoplasma.

Commonly misidentified lines (See <u>ICLAC</u> register)

No cell lines used are listed in the database of commonly misidentified cell lines.

Animals and other organisms

Policy information about studies involving animals; ARRIVE guidelines recommended for reporting animal research

Laboratory animals Female 6-10 week ICR (Institute of Cancer Research) mice were used in this study. The female Anopheles stephensi and Anopheles

Laboratory animals Female 6-10 week ICR (Institute of Cancer Research) mice were used in this study. The female Anople gambiae mosquitoes were raised in our laboratory and used in this study.

Wild animals This study collected field-caught female Anopheles sinensis mosquitoes. This study did not include other wild animals.

Field-collected samples

Blood-engorged field caught female An. sinensis mosquitoes were collected in three different regions of China, Tengchong in Yunnan (YN), Wuxi in Jiangsu (JS) and Dandong in Liaoning (LN). Mosquitoes were collected from house walls with a mouth aspirator and

reared in sterilized cups, and maintained at 26 \pm 2 °C and 70 \pm 5% relative humidity (RH).

Ethics oversight

All animal experiments followed the ethical regulations and were carried out in accordance with protocols approved by the CAS

Center for Excellence in Molecular Plant Sciences (Shanghai Institute of Plant Physiology and Ecology) Animal Care and Use

Committee and by the Johns Hopkins University Animal Care and Use Committee.

Human research participants

Policy information about studies involving human research participants

Population characteristics P. vivax blood samples were collected from patients older than 18 years.

Recruitment P. vivax infectious blood was collected from patients who provided written informed consent.

Ethics oversight The experiment was approved by the National Institute of Parasitic Diseases Ethics Committee (2015-010).

Note that full information on the approval of the study protocol must also be provided in the manuscript.

Note that full information on the approval of the study protocol must also be provided in the manuscript.